Analysis of Subatech cloud chamber images

Gilles GRASSEAU and Gines MARTINEZ

November 2023

Abstract

The aim of this internship is to understand the basic principles of a cloud chamber detector, to understand radioactivity and in particular the origins of natural radioactivity, to understand the basic principle of the radiation-matter interaction and to build an experimental system able to generate good quality digital pictures and films of the cloud chamber, to build a toy model for the response function simulation of the cloud chamber and finally to develop an analysis algorithm to identify alpha tracks in the cloud chamber and to measure the length and origin of the track.

1 Goals

- Radioactivity basic knowledge : nucleus quantum bound system, radionuclides, radioactivity, alpha decay
- Natural radioactivity, natural radionuclides, telluric radionuclides ^{238}U, ^{235}U, ^{232}Th and ^{40}K, decay chains of natural radioactivity
- Interaction radiation with matter : energy loss of non relativistic massive particle in matter
- Subatech cloud chamber. Realisation of a toy model simulation of the Subatech cloud chamber
- Installation of the Subatech cloud chamber. Realisation of picture and films of the Subatech cloud Chamber.
- Analysis of Subatech cloud chamber pictures : i) binary pixelisation of the pictures, ii) clustering algorithme, iii) calculations of basic properties of the cluster, iv) Identifications of alpha tracks, v) calibration procedure, vi) Measurement of the alpha track path-length and origin.

- Analysis of the Subatech cloud chamber film. Proposition of new ideas (measurement of the life time of Polonium, contribution of ^{235}U, measurement of radon radioactivity in the air, ...

2 Equipement

- Cloud chamber of Subatech
- Camera (camera professionnel ou camera iPhone ou web camera ordinateur Linux)
- Mechanical structure, to be designed, to support de camera
- 1 or 2 (in case of internship in pairs) of scientific linux computers to be installed in a Subatech office. One of the computer could be a laptop in order to open the possibility to easily take pictures and films of the cloud chamber with a web cam in the experimental room.

A Appendix A : Chaines de décroissance

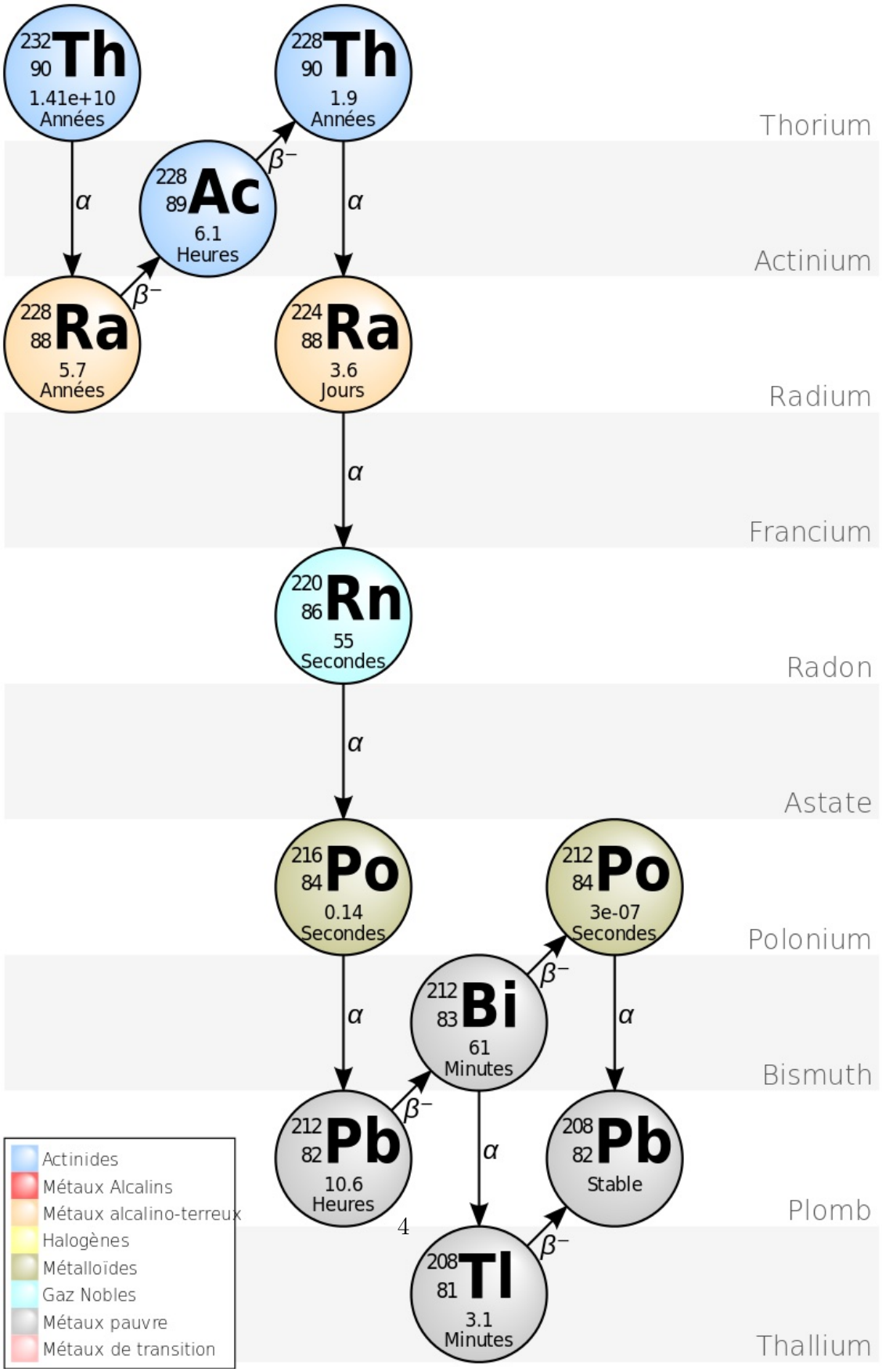

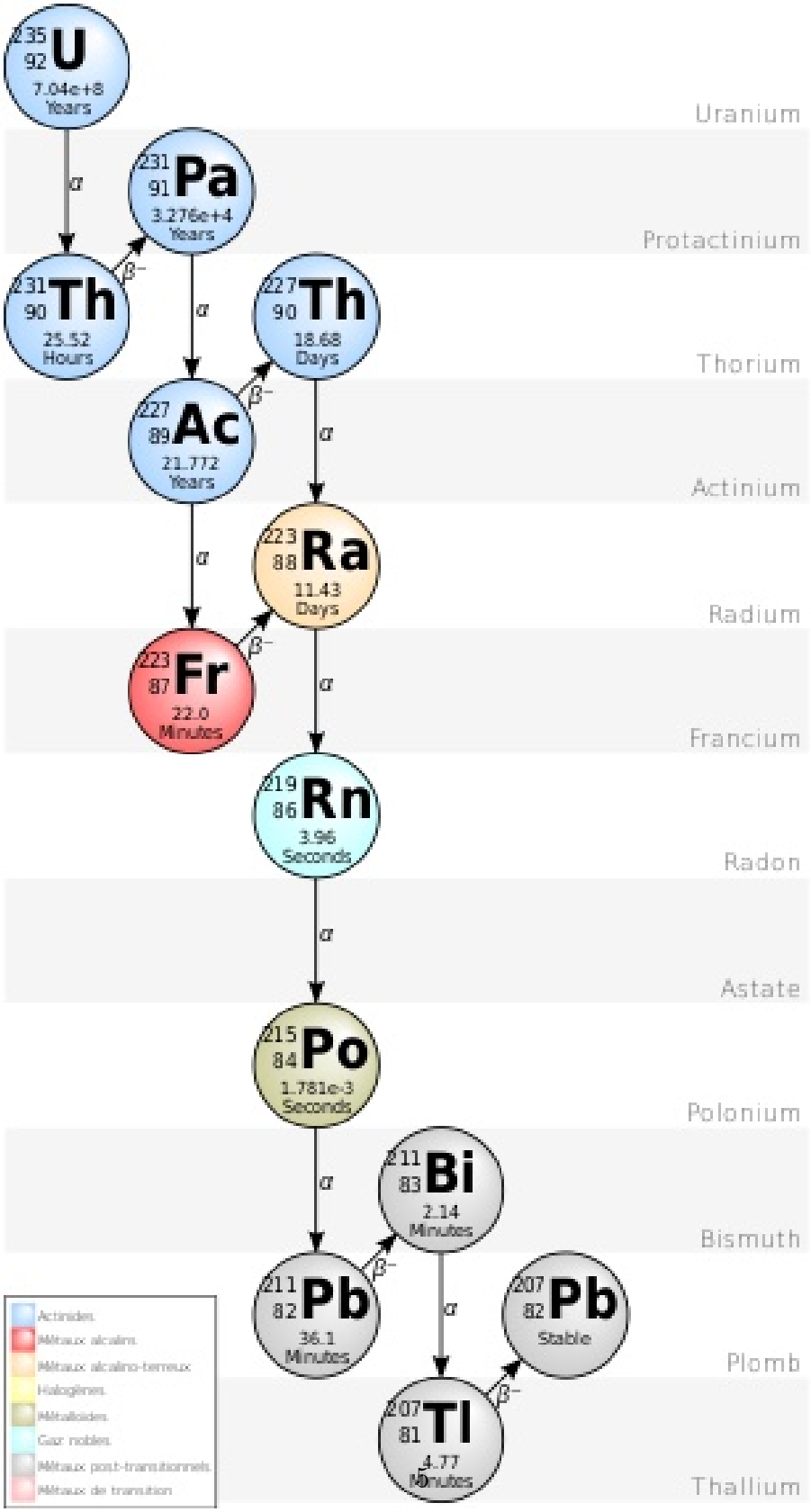
235 92 U 7.04e+8 Years
231 91 Pa 3.276e+4 Years
231 90 Th 25.52 Hours
227 90 Th 18.68 Days
227 89 Ac 21.772 Years
223 88 Ra 11.43 Days
223 87 Fr 22.0 Minutes
219 86 Rn 3.96 Seconds
215 84 Po 1.781e-3 Seconds
211 83 Bi 2.14 Minutes
211 82 Pb 36.1 Minutes
207 82 Pb Stable
207 81 Tl 4.77 Minutes
α
β−
Uranium
Protactinium
Thorium
Actinium
Radium
Francium
Radon
Astate
Polonium
Bismuth
Plomb
Thallium
Actinides
Métaux alcalins
Métaux alcalino-terreux
Halogènes
Métalloïdes
Gaz nobles
Métaux post-transitionnels
Métaux de transition

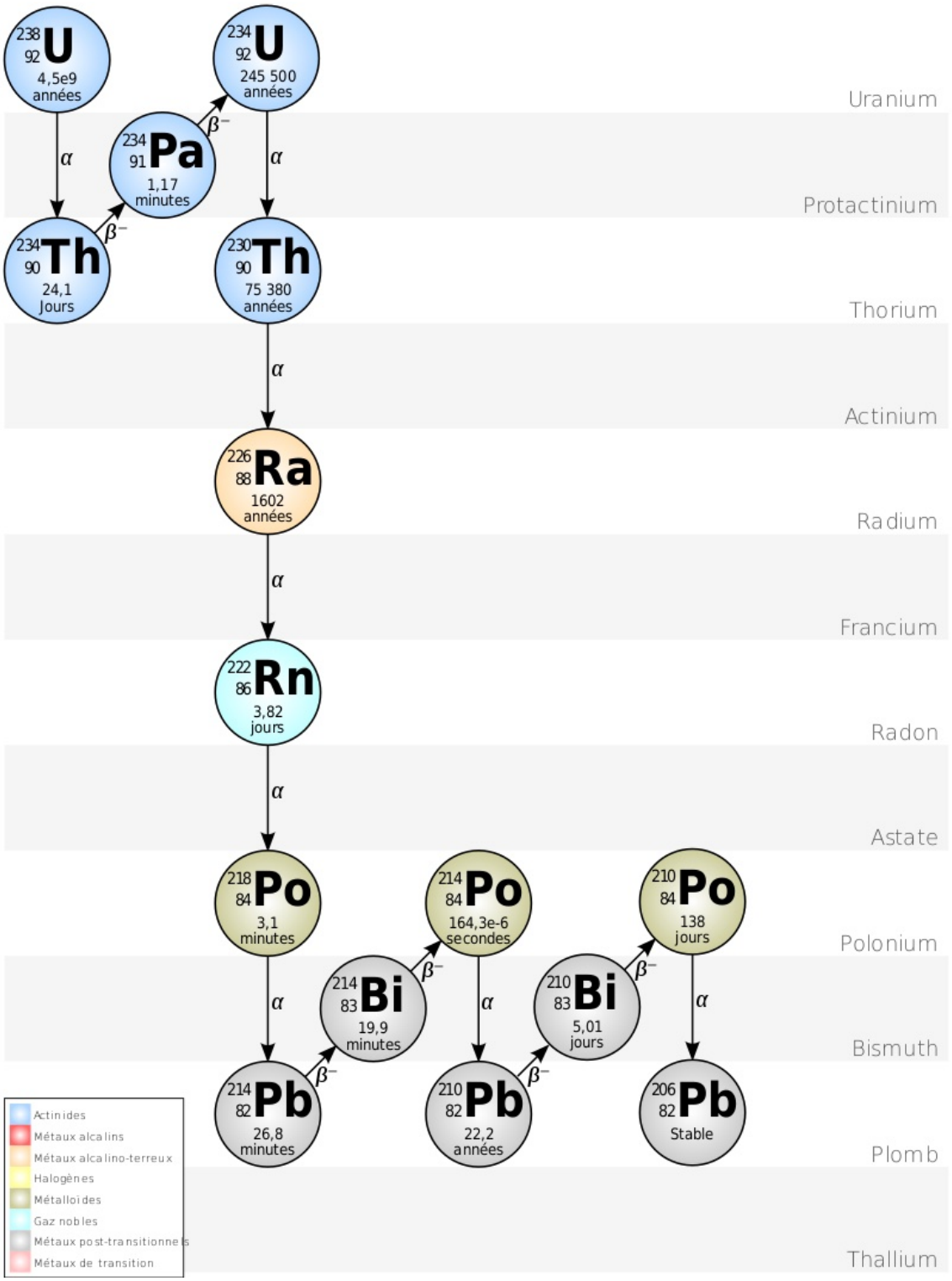
238 92 U 4,5e9 années
234 92 U 245 500 années
234 91 Pa 1,17 minutes
234 90 Th 24,1 Jours
230 90 Th 75 380 années
226 88 Ra 1602 années
222 86 Rn 3,82 jours
218 84 Po 3,1 minutes
214 84 Po 164,3e-6 secondes
210 84 Po 138 jours
214 83 Bi 19,9 minutes
210 83 Bi 5,01 jours
214 82 Pb 26,8 minutes
210 82 Pb 22,2 années
206 82 Pb Stable
α
β−
Uranium
Protactinium
Thorium
Actinium
Radium
Francium
Radon
Astate
Polonium
Bismuth
Plomb
Thallium
Actinides
Métaux alcalins
Métaux alcalino-terreux
Halogènes
Métalloïdes
Gaz nobles
Métaux post-transitionnels
Métaux de transition

B Appendix B : Grande chambre à nuage de diffusion PJ45/1

Grande chambre à nuage de diffusion PJ45/1

09046.90
09046.93
09046.98

Mode d'emploi

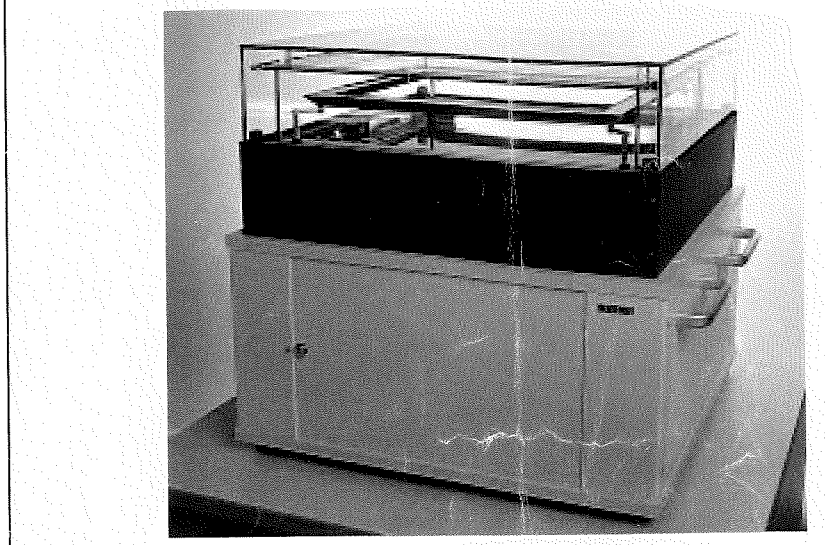

1 INTRODUCTION

Dans notre société, la radioactivité est un sujet qui depuis de nombreuses années joue un rôle prépondérant dans la politique, l'économie et les médias. Parce que cette radiation ne peut être perçue par nos sens naturels, et parce que ses effets n'ont pas encore tous été étudiés, elle réveille plus d'émotions que la plupart des autres sujets concernant les sciences.

Avec la chambre à nuage de diffusion de la Société Phywe Systeme GmbH, vous avez acquis un appareil qui permet de visualiser les traces de la radiation cosmique et terrestre. Les traces permettent d'identifier différents types de radiation naturelle, et les sources de radiation artificielles permettent d'effectuer des expériences en physique.

2 INSTALLATION ET FONCTIONNEMENT

La grande chambre à nuage de diffusion est constituée d'un socle de chambre et d'une chambre d'observation. Le socle de chambre contient la machine réfrigérante, l'alimentation électrique, le réservoir à alcool, la pompe à alcool et la minuterie; la chambre d'observation se trouve au-dessus du socle.

Le fond de la chambre d'observation est constitué d'une plaque métallique massive norcie (surface 45 x 45 cm), refroidie uniformément sur toute sa surface par la machine réfrigérante (environ -35 °C).

Le toit et les parois latérales de la chambre d'observation sont constitués par deux capots de verre superposés. Entre les deux capots est disposé un treillis de fins fils de chauffage (17), qui servent à réchauffer cette partie de la chambre, évitant de ce fait la formation de buée. Ce treillis sert également de grille de haute tension pour l'absorption des ions.

Dans la partie supérieure, sous le capot de verre, se trouve une rigole (15) chauffée électriquement qui contourne tout le capot et dans laquelle tombe goutte à goutte de l'alcool isopropyle d'un petit tube courbe (14).

L'alcool est évaporé et diffuse depuis le secteur supérieur chaud de la chambre vers le fond froid. L'alcool s'y condense et retourne dans le réservoir.

Au dessus de la mince couche de liquide couvrant le fond, il se forme un zone de vapeur d'alcool sursaturée. C'est dans cette zone uniquement que les particules de matière chargées venant de l'intérieur ou de l'extérieur génèrent des ions le long de leurs trajectoires. Des gouttelettes d'alcool isopropyle s'y attachent préférentiellement, formant la trace de brouillard visible pour l'observateur. La longueur et la constitution de la trace de particules permet de tirer des conclusions concernant la particule chargée.

3 INSTALLATION DE L'APPAREIL

Pour assurer à l'observateur une vue optimale, nous recommandons d'installer l'appareil sur une table, carrée de préférence, dont les côtés mesurent entre 90 et 100 cm. L'appareil pesant 80 kg, il faut veiller à ce que la table soit suffisamment robuste. La hauteur de la table devrait être de 60 cm environ. Nous recommandons la table Phywe 20001.03/2002.00; dont les pieds peuvent être réglés à la hauteur voulue.

Il faudra veiller à ce que les fentes d'aération (19) soient libres et que l'appareil ne soit pas trop exposé à la lumière directe venant d'en haut. Une pièce légèrement assombrie serait idéale.

Branchez la chambre à nuage au réseau à l'aide du câble de raccord fourni. La prise principale (1) se trouve à l'arrière, en bas. La prise de courant utilisée doit être protégée par un disjoncteur de 10 à 16 A.

La chambre à nuage de diffusion doit être réglée en position horizontale à l'aide des pieds de réglage (16), afin que le niveau d'alcool dans la rigole (15) soit uniforme, pour obtenir une image régulière.

4 MISE EN ROUTE

Le socle est accessible de deux côtés. Pour ouvrir ces deux côtés, on ouvre la serrure correspondante (2, 3), on déplace la paroi latérale avec serrure de quelques centimètres vers la droite et on soulève la plaque vers le devant pour la retirer.
Vous trouverez à l'avant (inscription "Cloud Chamber") un tableau de commande avec les éléments et commandes suivants:

- Réservoir à alcool (peut être retiré), avec double tuyau souple pouvant être dévissé (12).
- Interrupteur principal (4).
- Commutateur "Opération permanente - minuterie" (5).
- Commutateur "Haute tension" (6).
- Vis moletée pour l'alimentation en alcool (11).
- Bouton de réglage pour chauffage de la rigole (7).
- Minuterie (8).
- Disjoncteur automatique (9).

Après avoir raccordé l'appareil au réseau et ouvert la paroi avant, retirez le réservoir à alcool (12) de son alcôve et dévissez l'écrou d'accouplement (13) qui retient le double tuyau flexible. Remplissez le réservoir d'alcool, revissez les tuyaux et remettez le réservoir à sa place dans l'alcôve.
Mettez ensuite les commutateurs dans les positions suivantes:

Interrupteur principal (4)	ON
Mode (5):	utilisation permanente
Haute tension (6):	ON

Réglez maintenant le débit d'alcool dans la rigole d'évaporation (15) au moyen de la vis moletée (11). Tournez la vis moletée à gauche et observez le débit d'alcool provenant du petit tube courbé (14). Dès que le niveau d'alcool dans la rigole a atteint environ 1 cm, réduisez le débit à environ 2 gouttes par seconde. Le niveau d'alcool dans la rigole devrait rester sensiblement constant durant l'utilisation de l'appareil. Au bout de 5 minutes environ, les premières traces blanches devraient être visibles sur la plaque d'observation noire. Si les traces apparaissent laiteuses et diffuses au bout d'une heure de travail environ, baissez légèrement le chauffage de la rigole au moyen du bouton de réglage (7). Si les traces étaient trop faibles, augmentez le chauffage.
Si vous désirez laisser fonctionner la chambre à nuage en automatique, mettez les indices de la minuterie aux heures auxquelles vous désirez que la machine se mette en route chaque jour (marque rouge pour la mise en route / marque verte pour l'arrêt) et mettez le commutateur de mode (5) sur "Timer". Consultez le mode d'emploi de la minuterie pour de plus amples renseignements.
Refermez l'avant de l'appareil en engageant la paroi (3) du côté droit de l'ouverture, pressez pour fermer, poussez vers la gauche jusqu'à l'arrêt et refermez à clé.

Ouverture de l'arrière

La paroi arrière peut être ouverte de la même façon que la paroi avant. Vous verrez la machine réfrigérante, le thermostat et le voyant (21) pour le niveau du liquide réfrigérant. Durant l'utilisation, le voyant doit toujours être rempli de liquide, et il ne doit pas y avoir de bulles.
Le thermostat a été réglé à la valeur optimale en usine. En cas de températures ambiantes extrêmes, de légères corrections sont possibles en tournant le bouton situé à la partie supérieure du thermostat. Les réglages de la machine réfrigérante ne doivent être effectués que par du personnel expert.

Sources de radiation artificielles

Sources de radiation artificielles

Du côté gauche du socle, vous trouverez une ouverture (2) permettant l'introduction de sources de radiation artificielles. La plaque de fermeture peut être ouverte en la déplaçant vers la droite au moyen de la tête de vis. La sphère pourvue d'un pointeau qui se trouve derrière, peut être tournée au moyen du pointeau, jusqu'à ce que l'ouverture vers la chambre intérieure soit visible. Cette ouverture permet par exemple d'introduire la source de thorium Phywe de quelques centimètres à l'intérieur de la chambre.

Indications générales

La consommation d'alcool de la chambre à nuage est faible. Néanmoins, en cas d'utilisation permanente, ou en cas d'utilisation fréquente avec programme hebdomadaire, les réserves d'alcool et le débit d'alimentation en alcool doivent être vérifiés régulièrement.
Il faut absolument remplacer l'alcool avec du 2-propanol (alcool isopropyle).
Il est recommandé de nettoyer les capots de verre de temps à autre. Ceci peut être fait au moyen d'un produit commercial à nettoyer les carreaux. Le capot supérieur peut être soulevé pour le nettoyage.
S'il faut remplacer un lampe, il faut dévisser les tôles de revêtement. Le tournevis nécessaire est attaché devant la machine réfrigérante.
Voir la photo pour de plus amples renseignements.

Attention

Il ne faut jamais transporter la chambre à nuage (par exemple pour la changer d'emplacement) avec la rigole d'évaporation d'alcool pleine. La chambre à nuage a été pourvue entre-temps d'un robinet de vidange supplémentaire, permettant de vider la rigole d'évaporation d'alcool. Ce robinet est actionné au moyen d'un bouton de réglage qui se trouve au-dessus de la vis moletée (11) permettant de régler l'alimentation en alcool. L'ouverture du robinet de vidange fait que l'alcool retourne dans le réservoir (12). Une fois la rigole d'évaporation vidée, il faut refermer le robinet.

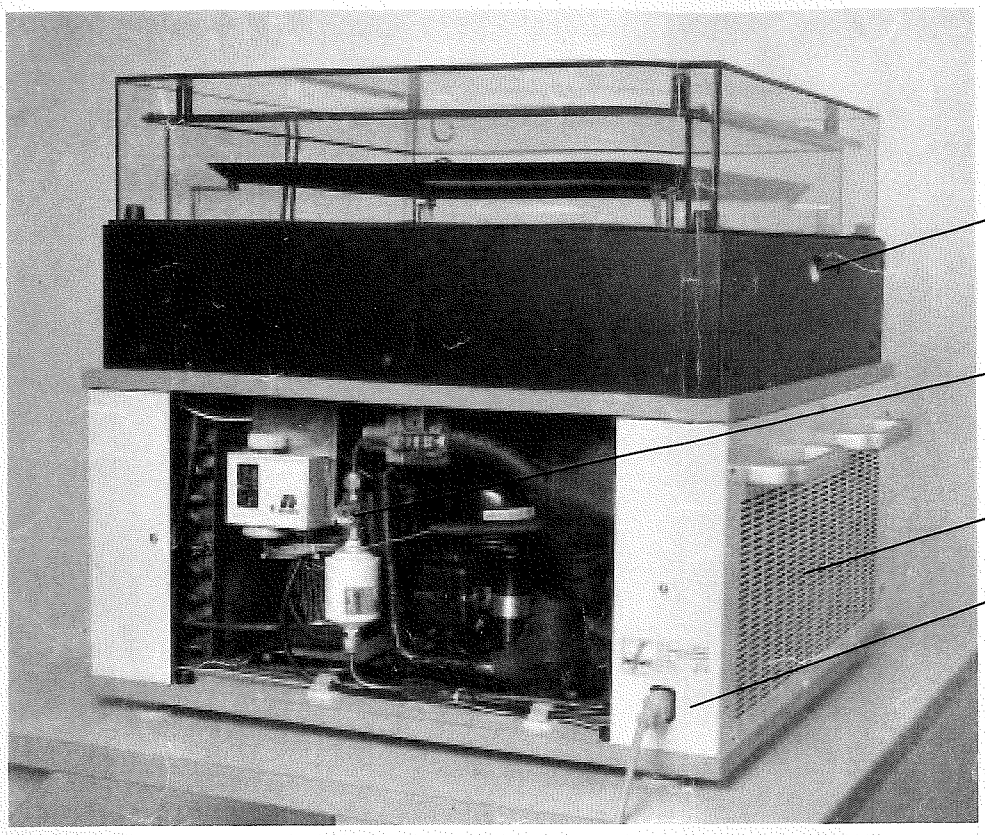

Rear view

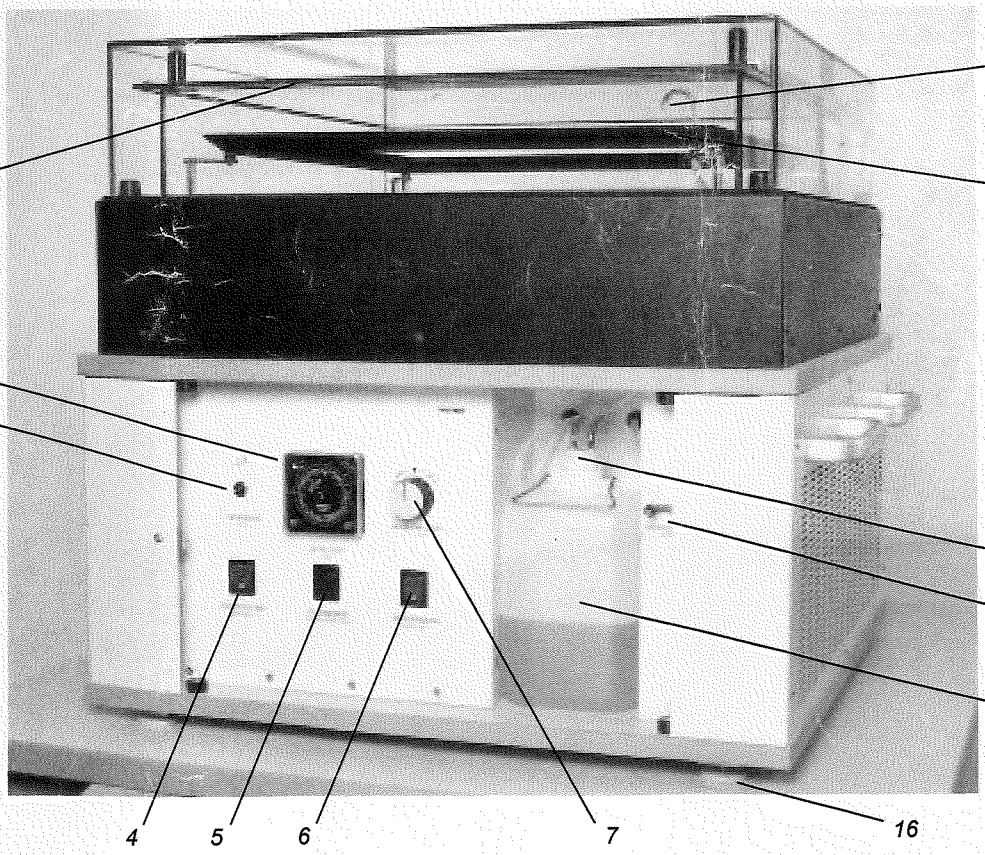

Front view

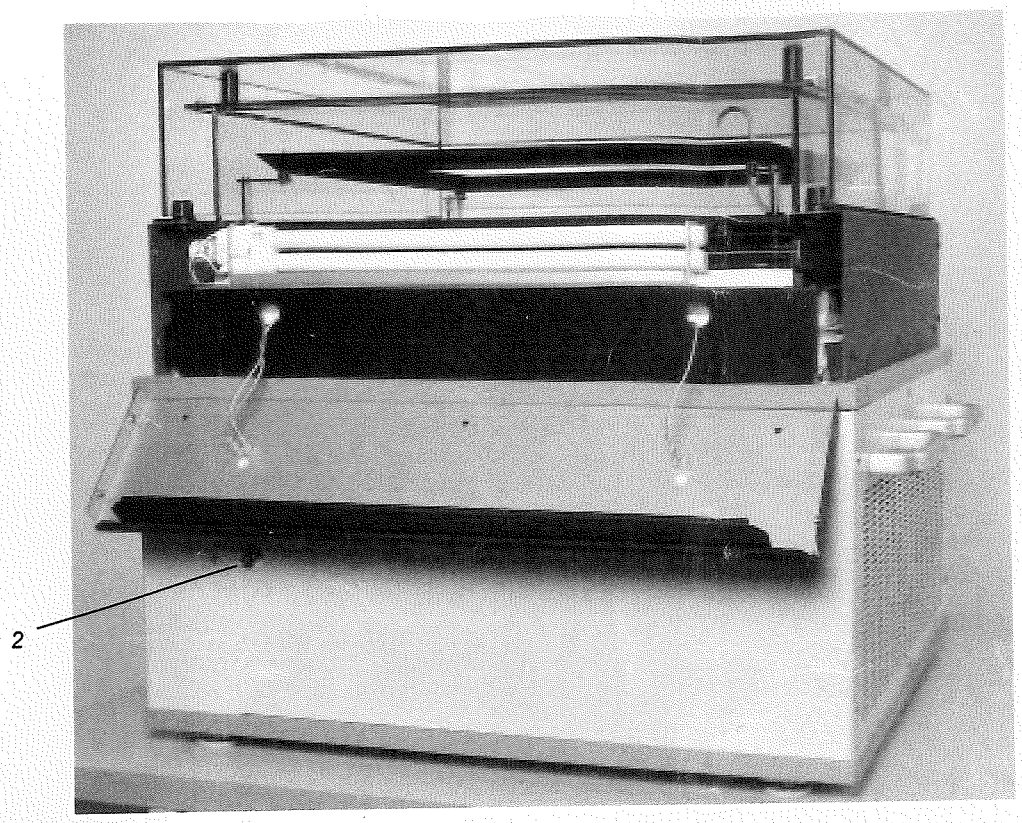

Illumination

5 SPECIFICATIONS TECHNIQUES

Couche active	45 cm x 45 cm x environ 1 cm
Chambre (l x p x h)	64 cm x 64 cm x 60 cm
Liquide de travail	2-propanol de haute pureté chimique (alcool isopropyle)
Volume du réservoir	2 litres
Eclairage	tubes fluorescents intégrés
Minuterie	7 x 24 heures (programme hebdomadaire)
Raccord au réseau	115/230 V, 50/60 Hz (prière d'indiquer à la commande)
Consommation de courant	0,9 kVA
Poids	80 kg

6 CHAMBRE À NUAGE ET ACCESSOIRES

Grande chambre à nuage de diffusion PJ45/1	09046.93
2-propanol, 1 litre	30092.70
Table pour chambre à nuage dimensions 90 cm x 90 cm x 78 cm (l x p x h)	
Bâti de table	20001.03
Dessus de table	20020.00

Sources radioactives artificielles sur demande.
Sous réserve de modifications techniques.

Valeurs de base pour la chambre à brouillard PJ 45

No. de l'appareil: _____

Ajustage du thermostat: _____

Chauffage gouttière: Aiguille sur point central

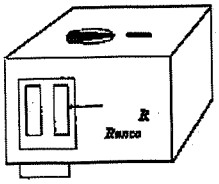

Apris avoir changé les valeurs de base, un changement visible est remarquable que après 30 minutes.

Natürliche Umgebungsstrahlung anschaulich sichtbar gemacht
Make natural background radiation permanently visible

Aufbau und Funktion

Die Nebelkammer besteht aus dem Kammersockel und der Beobachtungskammer.
Der Kammersockel enthält Kälteaggregat, Stromversorgung, Alkoholtank, Alkoholpumpe und Zeitschaltuhr, über dem Sockel befindet sich die Beobachtungskammer.

Den Boden der Beobachtungskammer bildet eine massive, geschwärzte Metallplatte (Fläche 45 cm × 45 cm), die durch das Kälteaggregat gleichmäßig über die gesamte Fläche gekühlt wird (etwa −30 °C).

Die Deckfläche und Seitenwände der Beobachtungskammer bestehen aus zwei übereinandergestülpten Glashauben. Zwischen den beiden oberen Glasscheiben befinden sich dünne Heizdrähte, die diesen Bereich der Kammer erwärmen und ein Beschlagen verhindern. Dieses Gitter dient gleichzeitig als Hochspannungsgitter zur Ionenabsaugung.

Im oberen Teil unter der Glashaube befindet sich eine umlaufende, elektrisch beheizte Rinne, in die aus einem Vorratsbehälter tropfenweise Isopropylalkohol gepumpt wird.

Der Alkohol verdampft und diffundiert vom oberen, warmen Bereich der Kammer zum kalten Kammerboden. Dort kondensiert der Alkoholdampf und fließt in den Vorratsbehälter zurück.

Oberhalb der dünnen, den Boden bedeckenden Flüssigkeitsschicht bildet sich eine Zone aus übersättigtem Alkoholdampf. In diesem Bereich, und nur hier, erzeugen geladene Materieteilchen, die aus dem Innenraum oder von außen kommen, längs ihrer Flugbahn Ionen[1]. An sie setzen sich bevorzugt Isopropylalkoholtröpfchen und ergeben die für den Beobachter sichtbare Nebelspur. Von der Länge und der Beschaffenheit der Teilchenspur kann auf das ionisierende Teilchen rückgeschlossen werden.

1) Bei der Ionisation trennt das einfliegende Teilchen Elektronen von den Gasmolekülen der übersättigten Dampfschicht ab, wodurch positive Ionen erzeugt werden. Die herausgeschlagenen Elektronen lagern sich an anderen Gasmolekülen an und bilden dadurch negative Ionen.

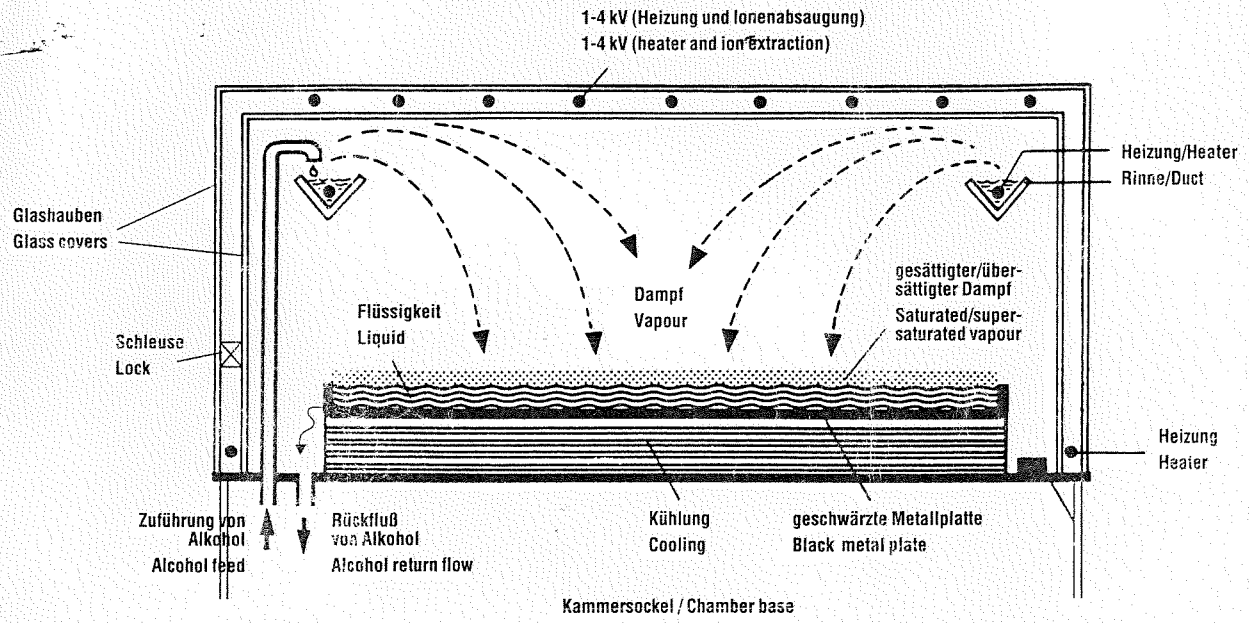

Diffusionsnebelkammer, Schnitt
Section through diffusion cloud chamber

Construction and function

The cloud chamber consists of the chamber base and the actual observation chamber. The chamber base contains the cooling unit, power supply, alcohol tank, alcohol pump and the time switch. The observation chamber is placed on top of the base. The bottom of the chamber consists of a solid, black metal plate (45 cm × 45 cm) which is uniformly cooled to about −30 °C over the whole area by the cooling unit.

The top surface and walls of the observation chamber are formed of two glass covers, one inside the other. Thin heating wires which serve for heating this region of the chamber to prevent condensation are located between the two upper glass panes. At the same time this grid is used as a high voltage grid for ion extraction.

The upper part of the glass cover is equipped with an electrically heated duct which extends around the whole circumference. Drops of isopropyl alcohol from a reservoir container are continuously pumped into the duct.

The alcohol evaporates and diffuses from the upper, warmer part of the chamber to the cold chamber bottom. Here the alcohol vapour condenses and flows back into the reservoir container.

A layer of supersaturated alcohol vapour forms above the thin layer of liquid covering the bottom. In this region, and only here, charged material particles coming from inside or outside the chamber produce ions along their flight path[1].
Isopropyl alcohol droplets become preferentially attached to the ions thus producing cloud tracks which can be observed. The type of ionising particle can be deduced from the length and nature of the particle track.

1) During ionisation the incoming particle separates electrons from the gas molecules of the layer of supersaturated vapour thus producing positive ions. The separated electrons become attached to other gas molecules to form negative ions.

C Appendix C : Visualisation of radioactive particle in a diffusion cloud chamber

Visualisation of radioactive particles / Diffusion cloud chamber

LEP 5.2.04

Related topics

α, β, γ-particles, β deflection, ionising particles, Mesons, cosmic radiation, radioactive decay, decay series, particle velocity, Lorentz force.

Principle and task

Radioactivity is a subject in our society which has been playing an important role throughout politics, economy and media for many years now. The fact that this radiation cannot be seen or felt by the human being and that the effects of this radiation are still not fully explored yet, causes emotions like no other scientific subject before.

The high-performance diffusion cloud chamber serves for making the tracks of cosmic and terrestrial radiation visible so that a wide range of natural radiation types can be identified. Furthermore, the diffusion cloud chamber offers the opportunity to carry out physical experiments with the aid of artificial radiation sources.

Equipment

Diffusion cloud chamber PJ45, 230 V	09046.93	1
Isopropyl alcohol, 1000 ml	30092.70	2
Thorium-source	09043.41	1
Radioactive source, Sr-90, 74 kBq	09047.53	1
Support base “PASS”	02005.55	1
Swinging arm	08256.00	1
Support rod, stainl. steel., 250 mm	02031.00	1
Right angle clamp “PASS”	02040.55	1
Object holder, 5 × 5 cm	08041.00	1
Holder for dynamometer	03068.04	1
Scale for demonstration board	02153.00	1
Accessory set for beta deflection	09043.52	1
Stand tube	02060.00	1

Problems

1. Determination of the amount of background radiation
2. Visualisation of α, β, γ-particles and mesons
3. Visualisation of the Thorium (Radon) decay
4. Deflection of β^--particles in a magnetic field

Fig. 1: Experimental set-up: Diffusion cloud chamber.

Setup and procedure

The cloud chamber consists of a chamber base and the observation chamber. The chamber base comprises a cooling element, a power supply, an alcohol reservoir, an alcohol pump and a programmable time switch. The observation chamber is placed onto the chamber base.

The bottom of the observation chamber is formed by a massive, black metal plate (surface 45 cm × 45 cm) which is cooled over the whole surface to about -30 °C by means of the cooling element.

The top plate and the side plates of the observation chamber consist of two glass hoods which are placed one into the other. A grid of fine heating wires is placed between the upper two glass plates. These wires serve for heating this area of the chamber thus keeping the hood free from condensation. At the same time they are held at high voltage thus generating an electric field that attracts the ions. The upper part of the glass hood includes an electrically heated gutter which runs around the whole circumference. Iso-propyl alcohol flows through a bended tube and drops into the gutter.

The alcohol evaporates and diffuses from the upper, warmer area of the chamber to the cold chamber bottom. There the alcohol is condensed into tiny droplets and flows back into the reservoir.

Right above the thin liquid layer covering the bottom a zone of oversaturated alcohol vapour is formed. It's in this area, and only in this area, that the charged material particles coming from the inside or from the outside produce ions along their trajectory. The tiny alcohol droplets preferably attach to these ions thus producing a visible cloud track. The length and the structure of the cloud track give information on the kind of ionizing particles.

In order to guarantee an optimum view on the observation chamber, it is recommended to place the chamber onto a square table (border length about 90 to 100 cm) which should be about 30-60 cm high.

Please make sure that the ventilating slots are not covered and that the cloud chamber is not subjected to direct light coming from above. A slightly darkened room whould be perfect. Use the connecting cable supplied to connect the cloud chamber to mains. The mains connection is located down on the back side. The corresponding mains socket should be protected for 10 A to 16 A.

Adjust the cloud chamber on an absolutely horizontal level with the aid of the adjustable feet in order to provide an even alcohol level in the gutter and thus a clear image.

When you have connected the cloud chamber to mains and opened the front side, remove the alcohol reservoir from its installation place and unscrew the union nut of the double tubing assembly.

Refill the alcohol reservoir, fix the double tubing again and place the reservoir back in place.

Now activate the switches as follows:

mains switch	ON
mode	continuous operation
high voltage	ON

The knurled nut serves for regulating the amount of alcohol dropping into the evaporating gutter. Turn the knurled nut to the left and observe the alcohol flowing through the bended tube and dropping into the gutter. When the gutter is filled to a liquid level of about 1 cm, reduce the alcohol supply to about 2 droplets per second. When the cloud chamber is being operating, the alcohol in the gutter should remain constant at this level. After about 5 minutes, the first white tracks should appear on the black observation surface. If, however, after 1 hour the tracks become a bit fuzzy and milky, you have to reduce the gutter heating by means of the control knob.

If the tracks are too weak, the heating of the gutter must be increased.

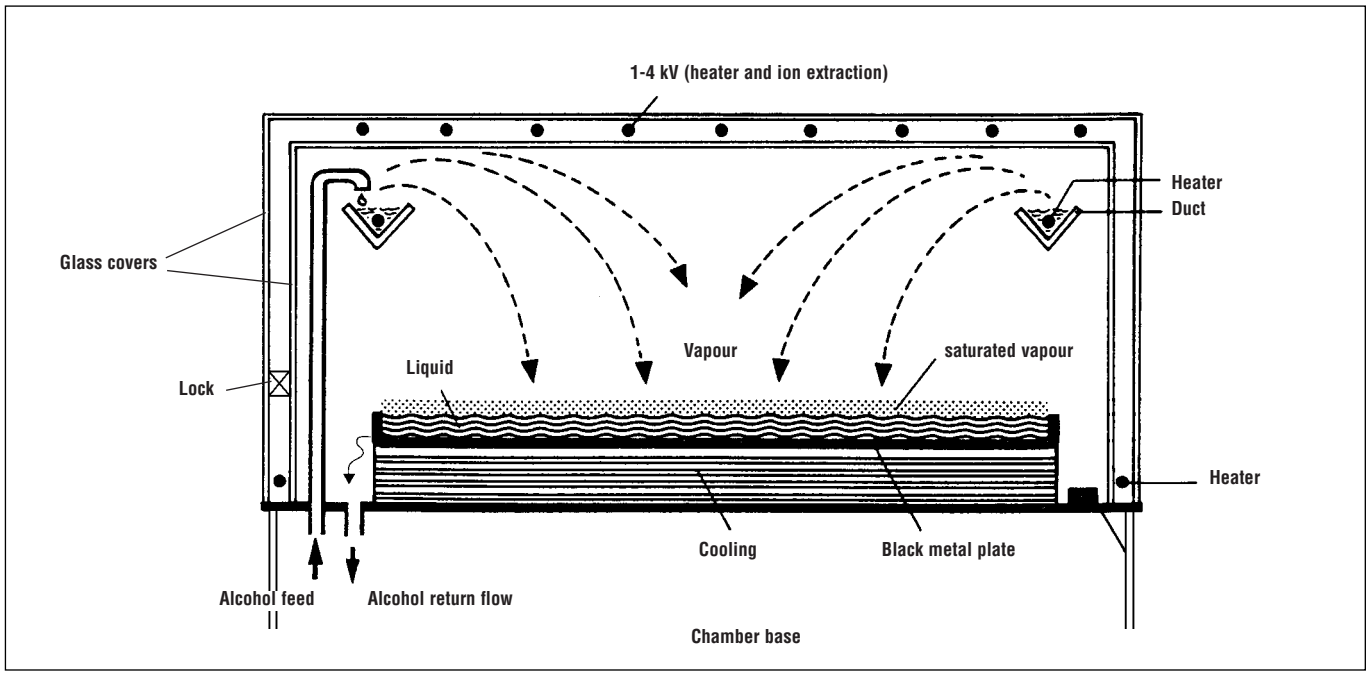

Fig. 2: Section through diffusion cloud chamber.

If you want to run the cloud chamber at automatic operation, set the markers of the programmable time switch to the desired switching time (red marker to switch the cloud chamber on, green marker to switch it off) and set the mode switch to “timer”. For more detailed information see the instructions on the programmable time switch.
Now close the front side by inserting the plate into the right side of the opening, pushing it back to the left stop position and locking it up.

Artificial radiation sources

On the left side of the chamber base there is an opening which serves for introducing artificial radiation sources. Use the head of the screw to push the plate to the right. The ball with pin which is located behind the plate can be turned around with the aid of the pin until the opening towards the inner area becomes visible. Now you can insert an artificial radiation source like, for instance, the thorium source a few centimeters into the inner area of the chamber.

Theory and evaluation

1. Natural Earth radiations

1.1 Cosmic rays

Radiations of particles with a high energy content (an exception: photon rays, which are electromagnetic waves) use to come from space down to every part of our terrestrial atmosphere (the primary cosmic radiations). Here are their main composition:

Particles	Percentage
protons	about 90 %
alpha-particles	about 9 %
bigger nuclei	up to 1 %

The particles penetrating into the atmosphere happen to bang into nuclei of the atmosphere and provoke nuclear reactions as well as nuclear splits. Therefore, new nuclei and elementary particles are created, go on flying and lead to other interactions.
In the atmosphere layers close to earth (less than 20 km high) one can observe only one secondary kind of radiations brought up by the numerous interaction-processes in the superior layers of the atmosphere. One must differentiate four kinds of components which have a different penetrating power (see Fig. 3):

Components of cosmic secondary rays	Components
Nucleons components	protons / neutrons
Electrons and photons components	elektrons / positrons / photons
Mesons components	measons of different charge
Neutrinos components	neutrinos / antineutrinos

In the Diffusion Cloud chamber, all particles charged in electricity can be detected, that is to say: electrons, positrons, mesons, protons and alpha-particles. Photons create only undirectly a trail when, by example, they eject an electron from

Fig. 3: Natural splitting processes.

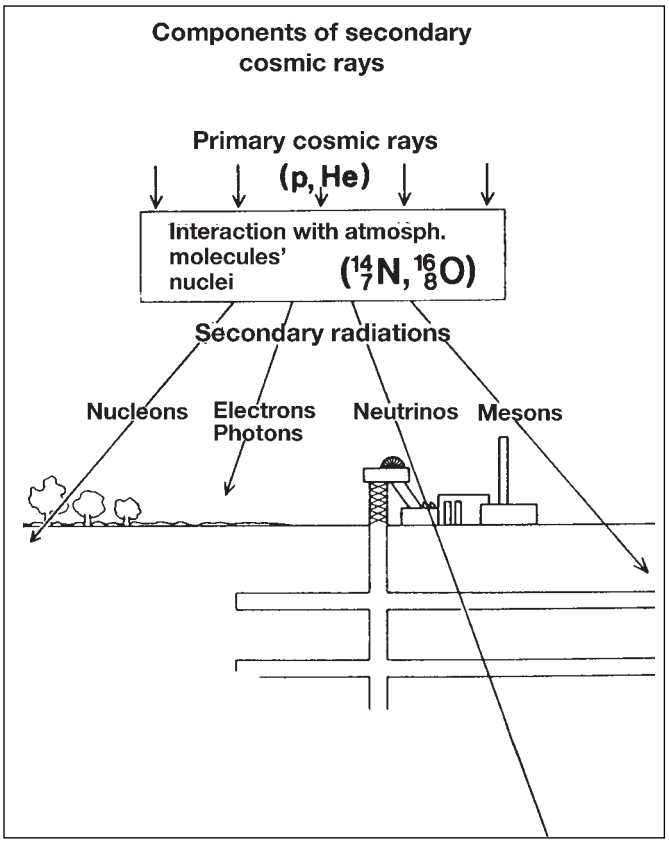

an atom, which produces a trail of ionisation. Neutrons can lead to nuclear reaction and then, the charged particle from the nucleus creates a trail:

Particles	Symbol	Relative mass	Charge	Radioactive Period
electron	e-	1	-1	stable
positron	e+	1	+1	stable
myon (μ- meson)	μ–	206.77	-1	$1.5 \cdot 10^{-6}$ s
myon (μ+ meson)	μ+	206.77	+1	$1.5 \cdot 10^{-6}$ s
proton	p+	1836.10	+1	stable
neutron	n	1838.62	0	11.7 mn
alpha-particle	α, He^{++}	7294.1	+2	stable

1.2 Terrestrial radiations

All materials on Earth (earth, water, atmosphere, animals…) contain natural radionuclides which send radiations. They have been existing since the creation of Earth (that is to say 4.5 thousand million years) or are constantly being created: U-238; Th-232; K-40 or Rb-87, for instance, belong to the natural radionuclides and have a very long radioactive period. Ra-226; Rn-222; Po-218 or Pb-210 are constantly being created and those radionuclides have a rather short radioactive period in the three natural splitting processes. There exist also natural radionuclides with a relative short-timed radioactive period, but these do not belong to the splitting process. They are constantly being created in the upper layers of atmosphere, such as C-14 from N-14 or H-3 from N-14 or O-16, for instance.

Fig. 4

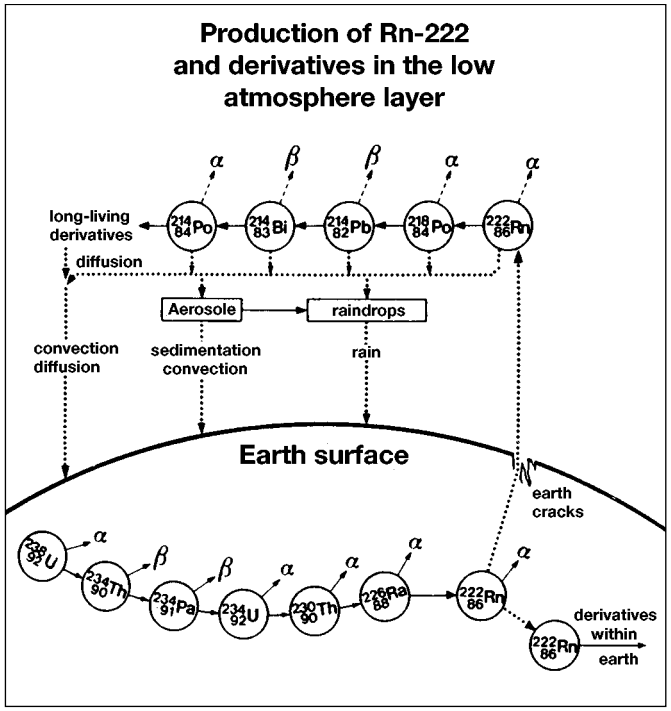

$$^{14}_{7}N + ^{1}_{0}n \rightarrow ^{14}_{6}C + ^{1}_{1}p$$

$$^{14}_{7}N + ^{1}_{0}n \rightarrow ^{12}_{6}C + ^{3}_{1}H$$

$$^{16}_{8}O + ^{1}_{0}n \rightarrow ^{14}_{7}N + ^{3}_{1}H$$

The about 100 natural radionuclides which have been existing since the creation of Earth or which are constantly being created can be found on the whole Earth in different concentrations. That is the reason why there are constant exchanges between earth, water, atmosphere and animal-life (Fig. 4).

That is why the Diffusion Cloud chamber is given materials made of natural radionuclides, which emit radiations.

2. The Diffusion Cloud chamber

How are tracks formed in the Cloud chamber?

The particles of which the radiation consists are unimaginably small. As an example, if we think of 1 trillion (1,000,000,000,000) protons lined up one after the other, they would only give a 2 mm long line! The particles in radiation can therefore not even be seen under the best microscopes.

Under certain conditions, however, the particles can produce cloud tracks which are visible to the human eye. Such tracks enable us to see where the particles have travelled. This is similar to looking at an aeroplane which is flying at a high altitude. The aeroplane itself is not visible from the ground, only the condensation trail can be seen.

Alpha particles, electrons, protons and mesons (each of the particles named carries an electrical charge) all produce cloud tracks in a cloud chamber. (The tracks of the individual particles look different, so that one can determine,

– which particle has flown through the cloud chamber,

– the speed at which it has flown (energy) and

– whether it had a collision or was deflected during its flight.

The alcohol vapour diffusing down from above to the black plate liquefies (condenses to drops), as soon as it reaches the immediate vicinity of the cooled plate.

Above the liquefied alcohol vapour, there is a 1–2 mm thick layer in which the vapour has just not quite liquefied. In this layer, drop formation, and so cloud formation, can be deliberately caused, e.g. by finest dust particles (condensation nuclei) or by a radiation particle flying through. During their flight, radiation particles “damage” (ionize) numerous alcohol molecules, which can then take on very much bigger alcohol drops and so become visible to us. They form the cloud track (Fig. 5).

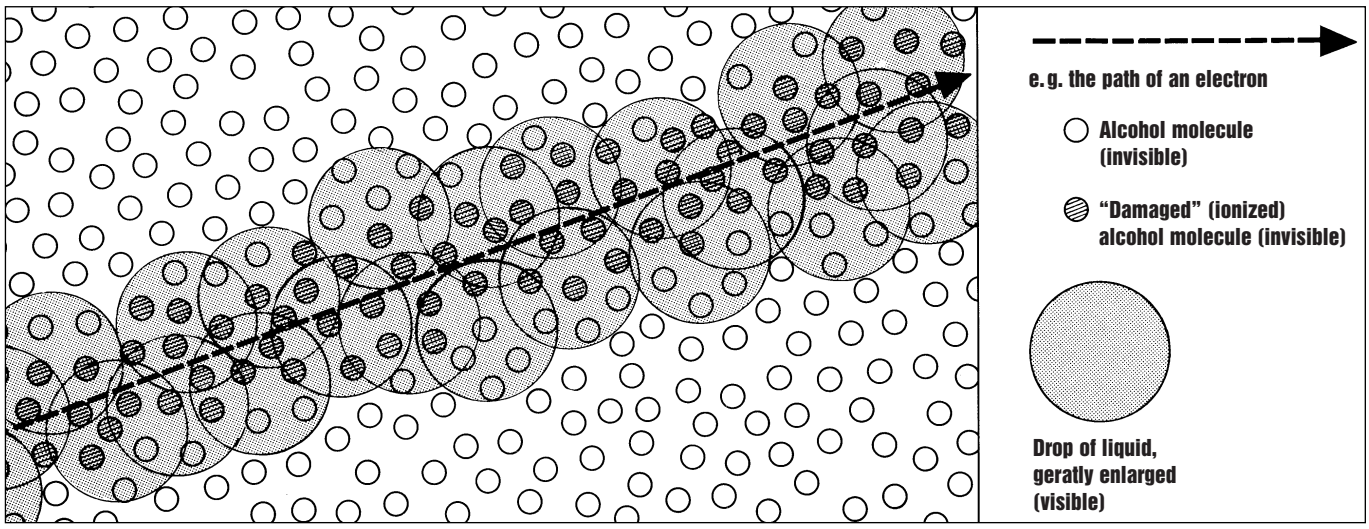

Fig. 5: The creation of cloud tracks in a cloud chamber.

Fig. 6: Track generated by an α-particle.

Fig. 8: Track generated by an electron with a high content of energy.

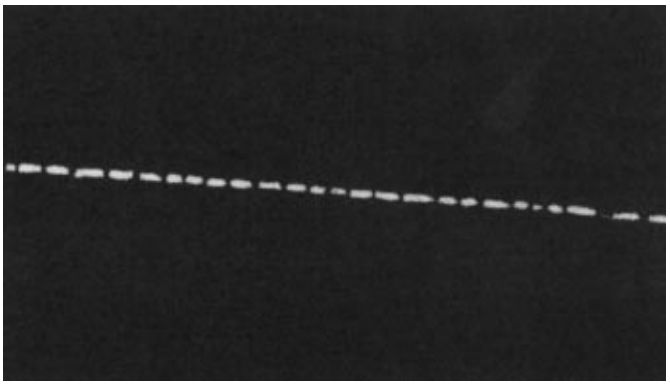

Problems

1. Determination of the amount of background radiation

All of the radioactive particles described in the previous chapter are continually present as so-called background radiation, unless one is in a special screened off room. When radioactive effects such as, for example, radioactive decay, are studied, then the zero rate resulting from the background radiation which was prevailing at that time must always be subtracted from the effects under observation. In general, the zero rate is about 18 registered impulses per minute. This measurement is usually made by means of a tube counter which is connected to a counting instrument. A glance at the active area of the cloud chamber shows, however, an apparently very great abundance of particles, which one tends to associate rather with the presence of a radioactive material in the chamber than merely to the background radiation. A little trick helps here to categorize the density of the particle tracks as really being due to background radiation.

Take a piece of typing paper and cut out a hole of about 0.8 cm diameter in the middle of it. Lay the piece of paper flat on the glass plate of the cloud chamber. Now, from a distance of about 10 cm from the paper, look through the hole with one eye and observe the active area of the cloud chamber. Count twenty "parts" of particle tracks which are visible through the hole and measure the time elapsed while doing so. This trick with the hole in the paper simulates the opening of a tube counter. Only those particles which hit the tube counter opening can be registered. From the multitude of particle tracks in the cloud chamber, only those are now visible which pass through an opening which corresponds to that of a tube counter. The zero rate which is theoretically to be expected can be so confirmed.

2. Visualization of α, β, γ-particles and mesons

In the chamber, one can observe tracks of "clouds" which are generated by α-particles, protons, electrons/positrons and mesons.

a) Example 1

Most of time, one can observe short tracks and thinner, longer tracks. To begin with, let us concentrate on short, but the biggest tracks (Fig. 6).

The appearence of α-tracks on the whole observation place is statistically dispersed, that is the reason why one cannot foretell when and where the next track will appear.

In the air, α-particles measure about 5 cm but in the steam of alcohol they are not longer. Moreover, α-particles can be absorbed by a single sheet of paper. How can they reach the interior of the Cloud chamber?

On the one hand, α-particles may have been liberated in the chamber itself by a radioactive nucleus. On the other hand, it may be protons with a high content of energy which were formed during the secondary radiations process in the atmosphere. They can penetrate into the chamber across the glas-protection. After penetrating the chamber, if their energy content is low enough as to being able to give their energy to the atom-electrons of the gas inside the chamber, they generate a track, which looks like the one of the α-particles (Fig. 7).

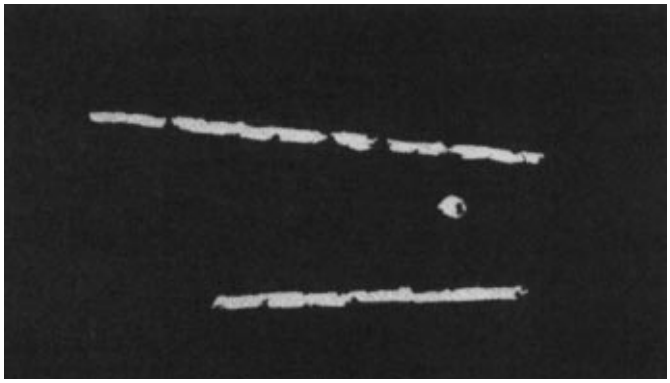

Fig. 7: Track generated by protons.

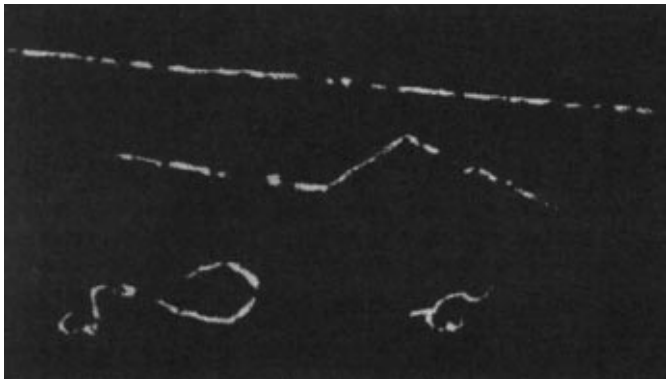

Fig. 9: Track generated by repeated deviated β-particle.

Fig. 10: Tracks of β-particles with a low content of energy.

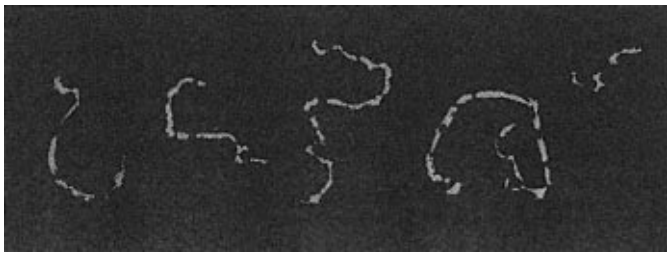

When the particle penetrate vertically the layer of supersaturated Alcohol steam, one can recognize only a spot as an ionisation trace.

b) Example 2

When the observer now observes the thin and to some extend very longer tracks (tracks with low drops density), one will be puzzled by the large amount of track manifestations. Therefore, we recommend you to consider precise forms – that is to say: the length of those tracks.

– First of all, observers should try to recognize a thin, straight and long trajectory – across the whole observation place. This shows particularly fast (with a high content of energy) electrons (Fig. 8).
– Slowly flowing electrons (i.e. with a low content of energy) have shorter trajectories, which are partly curved or buckled (Fig. 9) because of deviation.
– Electrons with a very low content of energy generate short trajectories, which look ornated or tortuous because of many deviations of the atoms in the steam layer (Fig. 10).
– Provided you place a powerful Ra-emitter, the γ-quanta will penetrate the chamber across the glas and release a large amount of photon-electrons or compton-electrons. Then, a formation of short and many times tortuous "worm-like" trajectories appears on the whole surface (Fig. 11).

c) Example 3

Mesons, which represent 90 % of the secondary cosmic rays can be detected in the Cloud chamber too. μ-mesons take an important part in this process since they have a positive or a negative elementary charge and their weight corresponds to 207 times electrons weight.
Mesons with a high content of energy create trajectories which look like tracks generated by electrons. However, high moderated mesons ionize highly and produce tracks which correspond nearly to those of α-particles. Therefore, it will be very difficult, in individual cases, to know whether one is being observing α-particles, protons, mesons or electrons (Fig. 12).
Since the average life-time of μ-mesons corresponds to micro-seconds, one can occasionally observe the dissociation of a μ-meson into an electron and into two invisible neutrinos in the Cloud chamber. The electron does not move to the same direction as the meson before, so that one can observe a characteristic bend in the track (Fig. 13). However, after the collision, one can clearly observe a thinner track, since the electron has a smaller ionisation density than the meson. The number of generated pairs of ions in each trajectory (in comparable conditions) are as follows:

– α-particles: 10.000
– protons: 5.000
– electrons: 100
– gamma-quanta: 1 (specific ionisation).

Fig. 12: Track generated by a meson.

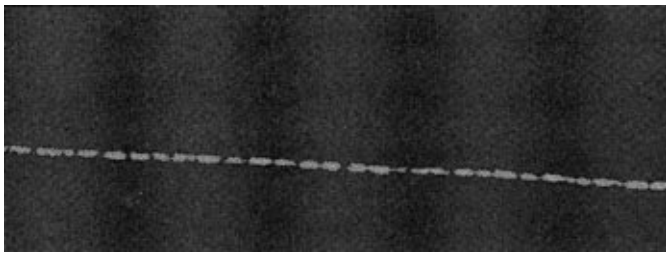

3. Visualization of Thorium (Radon) decay

The source (09043.41) contains a small quantity of a thorium salt (Th^{232}) which continually supplies radon gas (Rn^{220}), according to the decay chart (Fig. 14). Carefully blow it through the side opening of the cloud chamber by pressing the rubber bulb just once, and immediately close the opening of the cloud chamber. As soon as turbulence has abated, "V" shaped tracks are to be seen (Fig. 15).
On comparing these with the tracks described under point 2, it is clear that they are α particle tracks. The α particles all have the same energy, and should therefore produce tracks of the same length, but shorter and longer tracks can be clearly seen here. The explanation for this is that the α particles fly aross the active layer of the cloud chamber in various directions. Only those particles which fly parallel to the plate surface produce tracks of the maximum length. The shortest tracks – points – are produced when the layer is traversed vertically to the plate.

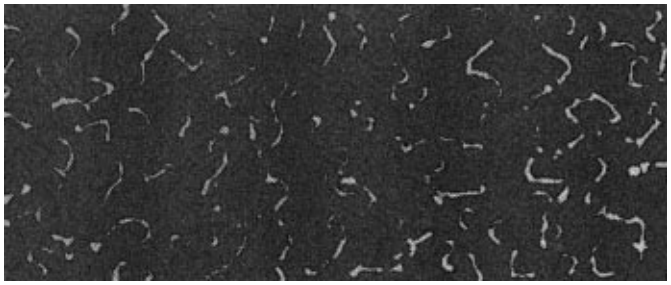

Fig. 11: Track generated by protons-electrons and compton-electrons.

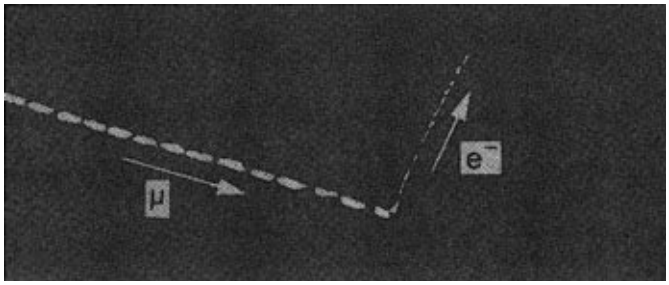

Fig. 13: Track of dissociation of a μ-meson into an electron and two neutrinos.

Thorium-decay series

Fig. 14

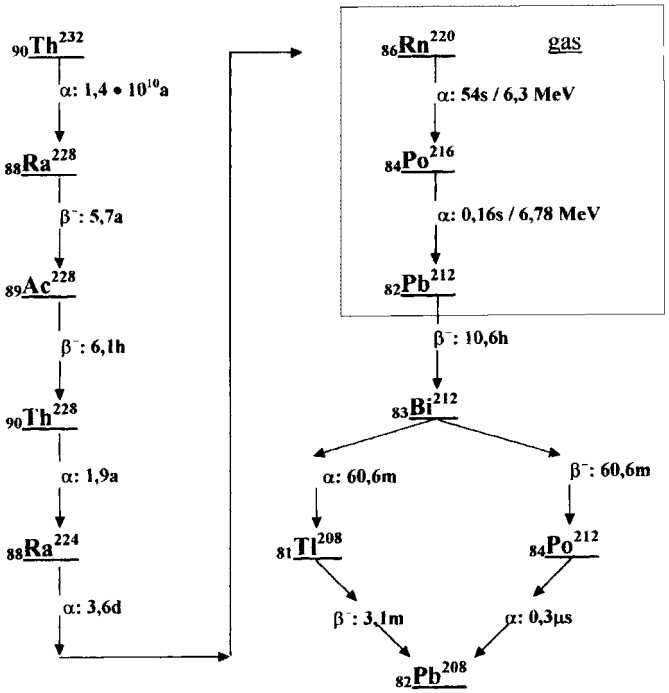

Fig. 15.

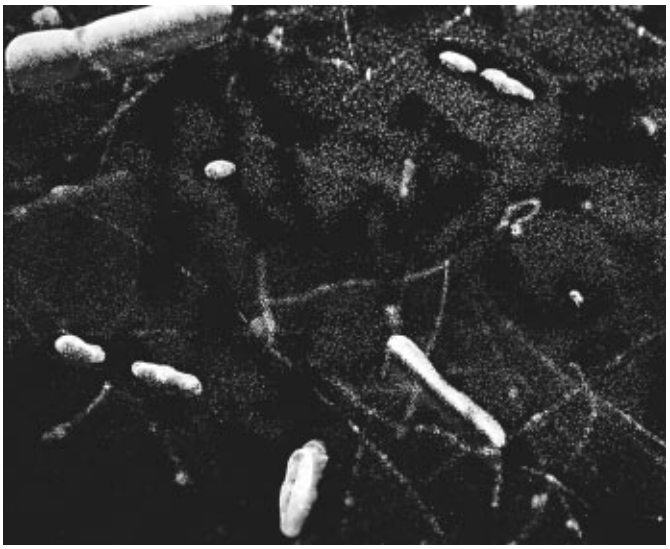

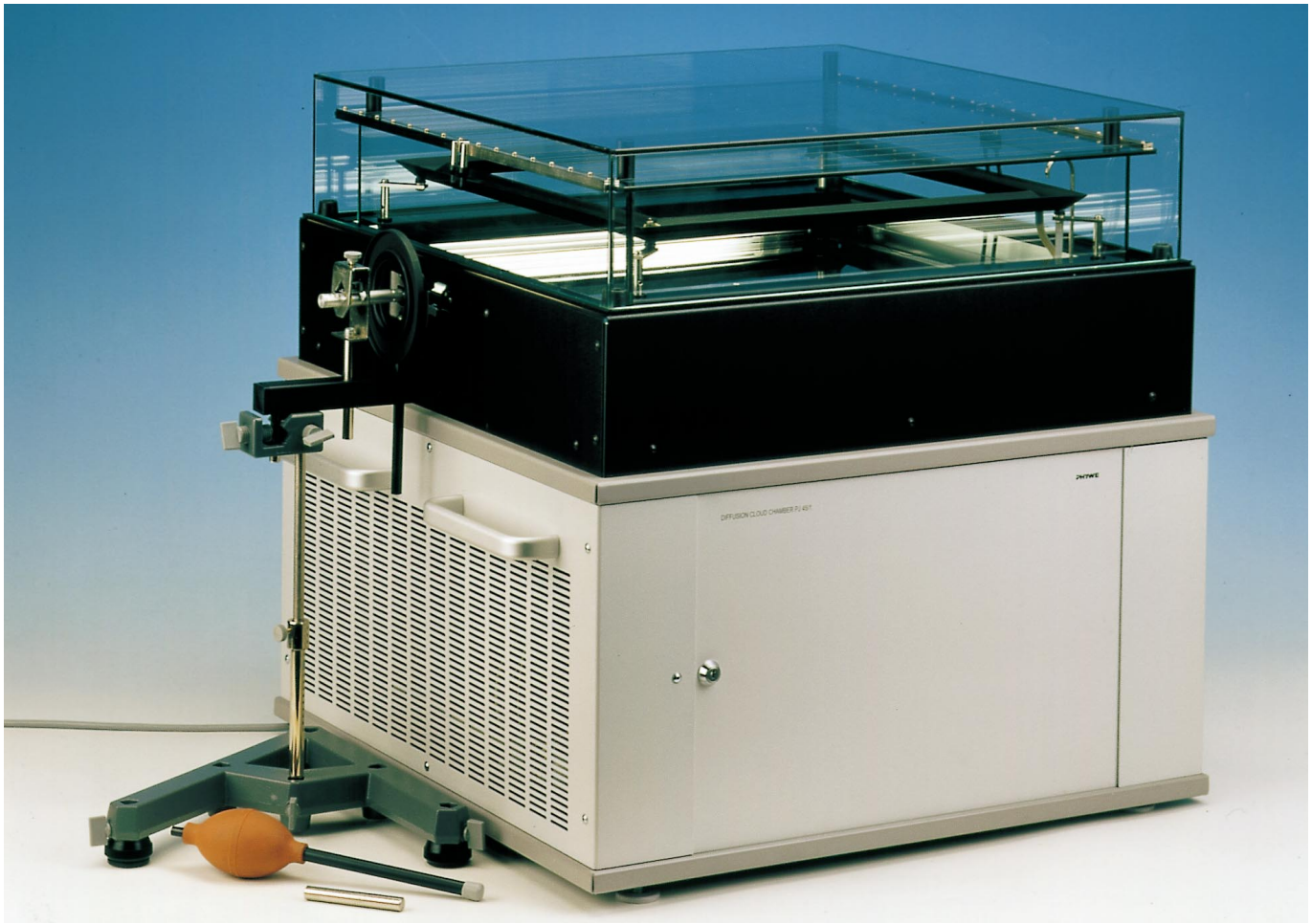

Fig. 16: Experimental set-up: deflection of β-particles.

Fig. 17: Details of the set-up for β-deflection.

Rn^{220} decays with a half-life of 54 s to Po^{216} which decays further, also under emission of α rays, with a half-life of 0.16 s to Pb^{212}. These two successive α decays are responsible for the "V" shape. As the two decay steps are not correlated to each other, there is no definite angle relationship between the α particles which fly apart. All "V" shapes, up to stretched out, linear ones, are to be observed.

On looking at them more closely, it can be seen that the branch of the "V" track is frequently not at the same position. Breaks in such tracks occur, which can up to a centimeter or so long. These interruptions in the tracks are due to the movement of the Po^{216} atoms, which do not themselves produce an ionized track. They have a half-life of about 0.16 s, and during this time they travel along the path where the track is interrupted. As soon as they emit an α particle, the track becomes visible again.

After about one minute, the number of "V"s in the cloud chamber is distinctly less, which confirms the half-life of 54 s.

Decays originating from Pb^{212} (Fig. 14) have essentially half-lives of from hours to minutes. They therefore do not contribute any further activity worth mentioning to the cloud chamber when Po^{216} has decayed. It should also be noted, that only relatively few radioactive atoms (Rn^{220}) were blown into the chamber (in principle, one could have counted them by counting the number of "V"s), to disintegrate there. The cloud chamber therefore again shows only the natural background radiation within a few minutes of the injection of Rn^{220}.

4. The deflection of β^- particles in a magnetic field

The set-up is as shown in Figures 16 and 17. Always use the metal dummy without specimen, not a pin with specimen, to adjust the height of the set-up and the rotatable magnet.

Fig. 18

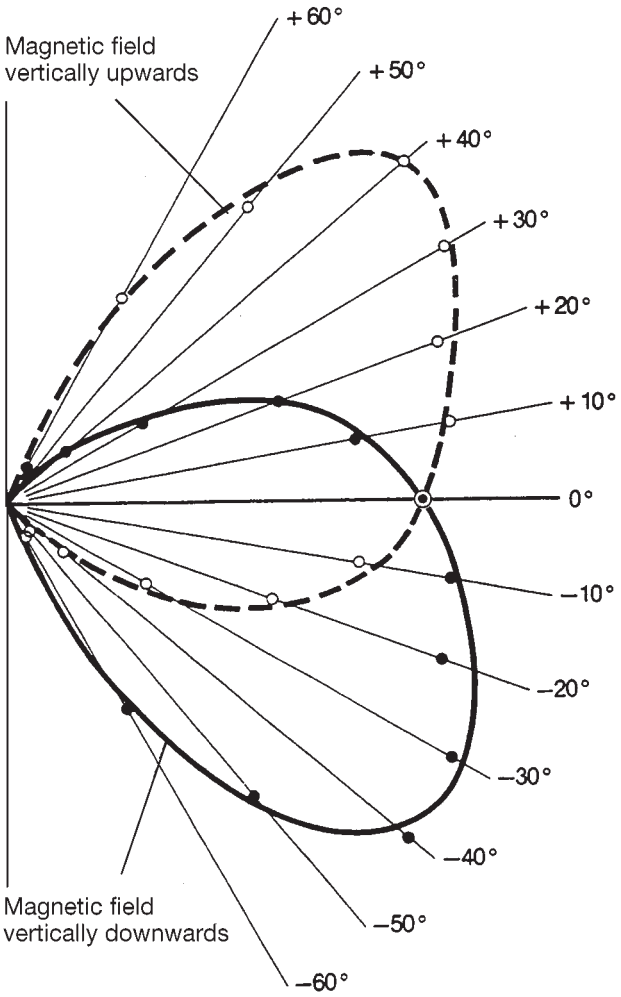

When a specimen pin is inserted, never look in the opening! Slide the active end of the Sr^{90} pin in the side opening of the cloud chamber and finely adjust the height, until distinct tracks can be seen in the chamber.

This experiment shows qualitatively, that the direction of the propagation of radiation from a Sr^{90} pin can be influenced by a magnetic field. Figure 18 shows the preferred direction of the β^- rays with two different magnetic field orientations. The area of maximum radiation intensity is at an angle which is distinctly different to zero. In the case of these β^- rays, we are dealing with moving electrons, which are naturally deflected in a magnetic field because of the Lorentz force. We can use the "right hand rule" to prove the negative polarity of the carrieres of charge (β^- rays, electrons). Hold the middle finger of the right hand in the direction of deflection (force direction) and the forefinger in the direction of the field (from the north pole to the south pole of the magnet, from red to green). Now spread your thumb out at 90° from the middle finger and forefinger, it points in the direction of the electric current associated with the movement of the carriers of charge. This movement is always towards the specimen. It is so clear, that negative particles must be radiated out from the specimen, as the "right hand rule" relates to carriers of positive charge.

The tracks in the cloud chamber show even more, however: Other than with α particles, which all have about the same energy, the β^- particles show a distinct energy spectrum, as on each disintegration, not only an electron but also an anti-electron neutrino is emitted, which also carries off energy. Because of this, the electrons, as they all have different speeds, are also deflected to different amounts by magnets. With the Sr^{90} specimen, the β^- radiation overlies even the γ radiation, which is not deflected by magnets but results in a widening of the club-shaped radiation in the 0° direction.

D Appendix D : Effect of the terrestrial radioactivity on the temperature of inside the Earth

Let us assume the Earth as a uniform sphere of iron oxyde (FeO) with a thermal conductivity of κ=2 W(m K) and let us assume a heat production uniformly distributed in the volume of the sphere with a value Q. The temperature distribution $T(x, y, z)$ inside the sphere must verify the following equation :

$$Q = -\kappa \Delta T(x, y, z) \tag{1}$$

Thermal isotropie of the considered matter and the spherical symmetry of the volume, imply that the temperature in the volume should be only function of the radius ρ from the center of the sphere : $T(\rho)$. Using spherical coordinates, the Laplacian is written as :

$$\frac{Q}{\kappa} = -\Delta T(x, y, z) = \frac{1}{\rho^2}\frac{\partial}{\partial \rho}\left(\rho^2 \frac{\partial T(\rho)}{\partial \rho}\right) = \frac{1}{\rho}\frac{\partial^2(\rho T)}{\partial \rho^2} \tag{2}$$

and in consequence :

$$\rho T(\rho) = -\frac{Q}{\kappa}\frac{\rho^3}{6} + T_{in}\rho + K \tag{3}$$

as the temperature should not diverge at $\rho = 0$, necessarily, $K = 0$:

$$T(\rho) = -\frac{Q}{\kappa}\frac{\rho^2}{6} + T_{in} \tag{4}$$

if one assumes that the value of the temperature on the surface of the sphere fo radius R, $T_{out} = T(R)$, is known and equal to 15 degrees Celsius, as in the Earth :

$$T(R) = -\frac{Q}{\kappa}\frac{R^2}{6} + T_{in} = T_{out} \tag{5}$$

where T_{in} which represents the temperature in the center of the sphere :

$$T_{in} = T_{out} + \frac{Q}{\kappa}\frac{R^2}{6} \tag{6}$$

If R=6300 km and assuming a natural radioactivity of the Earth similar to that of the human body, about 10^5 Bq/m^3 and a deposited energy per decay about 1 MeV, the radioactive heat density is about $Q = 10^5$ Bq/m^3 x 1 MeV = 10 nW/m^3, we obtain that :

$$T_{in} = 15 + \frac{10^{-8}}{2}\frac{6.3^2 10^{12}}{6} \tag{7}$$

and therefore the expected temperature in the center of the sphere is very high, although the heat density due to natural radioactiviy is very small, only 10 nW/m^3.

Reality is indeed much more complex than this scholar exercice :

1. Convection should be the most important mechanism for heat transport inside the Earth;
2. Thermal conductivity is not homogenious;
3. Natural radioactive heat is not homogenious
4. The amount of natural radioactivity and its distribution inside the Earth is not known
5. We do not know if the Earth heat exchange is stationary or if Earth is cooling down

E Appendix E : Computing code

The developed code is available in GitHub (this is the link to the computing code of this internship in GitHub).

First of all, in the README file you will find relevant and updated information.

The software SRIM is recommended for the calculation of the energy lost and path-length of alpha particles in matter (this is the url link) But it is more important that students are able to perform the calculation theirselves using the reference book W.R Leo (see bibliographie section, and in particular equaitons 2.26 in the book)

The computing python code traceSimulation.py (developed by Wassim and Ouassid in 2023, L3 students) performs a simulations of the projection length of the particule tracks in the detection plane of the cloud chamber, assuming a constant length of the track in 3D and an isotropic alpha decay. A simulation of this phenomena using geant4 would be a honourable objective but beyond the scope of the present internship for L3 bachelor level.

The computing code processing.py (developed by Gilles Grasseau) allows the identifications, reconstructions and mesure of the alpha track seen by the cloud chamber and acquired by a webcam.

The computing codes webcam_dacq.py et sPhone_dacq.py developed by Giles Grasseau allow for the acquisition of a photographe series with 1 second exposition per picture.

F Appendix F : Measuring radon concentration in air using a diffusion cloud chamber

R. Cases, E. Ros and J. Zúñiga, American Journal of Physics 79, 903 (2011); doi: 10.1119/1.3591320

Measuring radon concentration in air using a diffusion cloud chamber

R. Cases,[a] E. Ros,[b] and J. Zúñiga[c]
IFIC, University of Valencia—CSIC, 22085 Valencia, Spain

(Received 10 December 2010; accepted 25 April 2011)

Radon concentration in air is a major concern in lung cancer studies. A traditional technique used to measure radon abundance is the charcoal canister method. We propose a novel technique using a diffusion cloud chamber. This technique is simpler and can easily be used for physics demonstrations for high school and university students.
[DOI: 10.1119/1.3591320]

I. OVERVIEW OF DIFFUSION CLOUD CHAMBERS

A good overview of diffusion cloud chambers (also called permanent cloud chambers) is given in Ref. 1. In spite of important results obtained by typical (non-permanent) cloud chambers, also known as Wilson chambers, they have the limitation of being active only for brief intervals due to dead time typically exceeding 90%. This disadvantage is partly removed for cosmic ray analysis by triggering on the cosmic rays themselves, as discussed, for example, in Ref. 2.

To construct a permanently sensitive cloud chamber, it is best to use a supersaturated vapor, produced continuously rather than in cyclic adiabatic expansions as for Wilson chambers. This use yields excellent results. It was pioneered by Hoxton using air,[3] investigated by Vollrath using HCl and water,[4] and by Langsdorf,[5] who found the most successful approach. He used methanol as the vapor that diffuses vertically downward through a permanent gas (CO_2 or air) from the upper heated part of the detector to the bottom plate cooled by dry ice (solid carbon dioxide). The vapor was condensed at the bottom plate, and in the intermediate region between liquid and gas there was a methanol layer permanently sensitive to charged particle tracks. Langsdorf proposed a theory for the functioning of the chamber, namely, liquid droplet formation in the supersaturated layer and vertical heat diffusion and transfer. Schutt[6] improved this analysis. In particular, he calculated that the formation of a supersaturated vapor layer requires a temperature gradient between the top and the bottom of the chamber of at least 3.6°C/cm in an air–methanol mixture at 1 atm. The same conclusion holds for hydrogen alone provided that the pressure is increased to 10 atm. The minimum gradient increases with pressure, and is 6.3°C/cm for air–methanol at 3 atm, or hydrogen at 30 atm.

The Langsdorf apparatus is not simple, and published track photos[5] were of poor quality (worse than those obtained with the Wilson chamber). These limitations explain the long time before diffusion cloud chambers attracted real interest. Around 1950 some experimentalists, in particular Cowan,[7] learned how to build a simple apparatus, and recorded tracks with better quality than those obtained with the Wilson chamber. Diffusion cloud chambers were used widely in nuclear and particle physics until they were replaced by the more powerful bubble chambers at the end of the 1950s (see Ref. 1 and references therein). They are still used for demonstration purposes. As we will discuss, the diffusion cloud chamber is a compelling demonstration tool because it is the simplest possible detector that allows the observation of cosmic rays at the surface of the Earth.

As an example of their use in particle physics, we will describe the diffusion cloud chamber constructed by Schutt and coworkers,[8] which was exposed to pion beams at the Brookhaven National Laboratory Cosmotron and yielded an important result. The apparatus was a high pressure diffusion cloud chamber working with hydrogen at 21 atm and filled with methanol vapor. The top and bottom temperatures were $+20°C$ and $-65°C$, respectively. The detector was later upgraded and reached a diameter of 41 cm, operating in a magnetic field of 1.05 T. This detector was exposed to a secondary pion beam of 1.5 GeV/c, and ten events such as the one shown in Fig. 1 were recorded.[9] These events can be interpreted as interactions of the type $\pi^- p \rightarrow V_1 V_2$, where V_1 and V_2 are particles with V-shaped decays. These decays were identified as Λ and K^0, decaying according to $\Lambda \rightarrow p\pi^-$ and $K^0 \rightarrow \pi^+\pi^-$. Note that tracks are only associated with charged particles, and therefore neutral particles such as K^0 or Λ leave no tracks. This event was the first experimental observation of strange particles produced in pairs, consistent with theory.[10,11]

II. ATMOSPHERIC RADON

The abundance of noble gases in nature decreases rapidly with atomic number. Table I displays the noble gas abundances in Earth's atmosphere.

As shown in Table I, argon is by far the most abundant noble gas, followed by neon and krypton. In particular, argon abundance is increased by β decays of ^{40}K (this isotope is very common in the Earth's crust). In contrast, the abundance of xenon is surprisingly small, a fact that is not well understood. Abundances of radon vary a lot according to location. Radon is produced inside Earth's lithosphere by α decays of radium. Radium shows up in the uranium decay chain. For isotope ^{238}U, for example, we have the following decay chain:

$$^{238}\mathrm{U} \rightarrow ^{234}\mathrm{Th} \rightarrow ^{234}\mathrm{Pa} \rightarrow ^{234}\mathrm{U} \rightarrow ^{230}\mathrm{Th} \rightarrow ^{226}\mathrm{Ra} \rightarrow ^{222}\mathrm{Rn}, \quad (1)$$

with a ^{238}U half-life of 4.5×10^9 years and a ^{226}Ra half-life of 1600 years. Some estimates are that one square mile of Earth's surface with 6 in. depth contains 1 g of radium, and the entire Earth's surface liberates radon into the Earth's atmosphere at a rate of 90×10^{12} Bq per year.[12] The average radon concentration inside Earth's atmosphere is 6×10^{-19} atoms per air molecule, or equivalently 20 atoms/mL. Radon is the main cause of radioactivity in air. Its three isotopes are ^{219}Rn, ^{220}Rn, and ^{222}Rn. They appear in the decay chain of

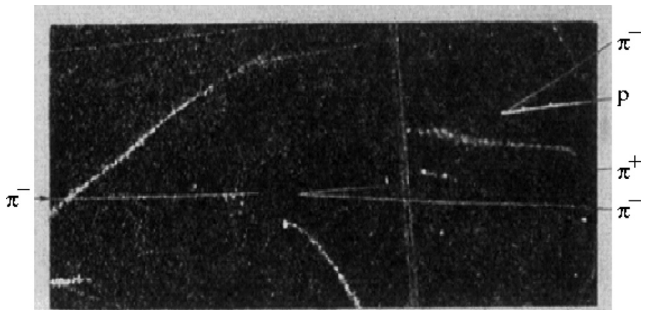

Fig. 1. Production of a pair of V-particles in the collision of a negative pion from the Cosmotron at Brookhaven National Laboratory and a proton at rest. This event can be interpreted as $\pi^- p \rightarrow K^0\Lambda$. Reprinted photograph from Ref. 9 with permission from The Physical Review. Copyright (1954) by the American Physical Society. http://prola.aps.org./abstract/PR/v93/i4/p861_1.

^{235}U, ^{232}Th, and ^{238}U, respectively. Their half-lives are 3.9 s, 55.6 s, and 3.8 days, respectively, and hence only the third isotope can be released significantly from the ground, and is relevant for measurements we will discuss. Radioactivity in air due to radon amounts to ≈ 20 Bq/m^3 in open air, increasing up to ≈ 100 Bq/m^3 in confined areas, although there may be much larger concentrations in localized areas.

Radon decays are believed to be the main cause of lung cancer. About 21,000 cases per year are recorded in the U.S., all of them directly or indirectly related to radon.[13] The risk is not due to gaseous radon, but to metallic solid daughters, namely lead and polonium, which stick to dust particles in air or smoke and stay inside the lungs. Smoking increases the cancer risk dramatically, both for smokers and nearby people. This theory about the origin of lung cancer is speculative.

Some interesting measurements on radon concentrations in Sweden can be found in Ref. 14. At 1 m depth below the Earth's surface, measured values are up to 40,000, 50,000, and 120,000 Bq/m^3 for moraine, sand, and clay soils, respectively.[14] For air the measured average value inside the House of Science of Stockholm is 220 Bq/m^3, varying from the usual 40 Bq/m^3 during day time, to as much as 700 Bq/m^3 when the ventilation was turned off at nights or during the weekends.

There are several techniques available for radon detection. One method used frequently (in particular for the measurements we have mentioned) is the activated charcoal canister method. This method makes use of a container with a filter and activated charcoal. Radon is absorbed by charcoal and after a few days exposure, the container is analyzed with a γ-spectrometer (NaI crystal for example) to detect photons from ^{214}Pb and ^{214}Bi, both daughters of ^{222}Rn. After correcting for various factors such as decay branching fractions and humidity, the average concentration of ^{222}Rn is estimated. Less sophisticated techniques are described in Refs. 15 and 16.

Table I. Noble gas abundances in the Earth's atmosphere in ppm (parts per million) of volume.

Noble gas	Z	Volume (ppm)
Helium	2	5.20
Neon	10	18.2
Argon	18	9340
Krypton	36	1.1
Xenon	54	0.09
Radon	86	$[0.1-18]\times 10^{-12}$

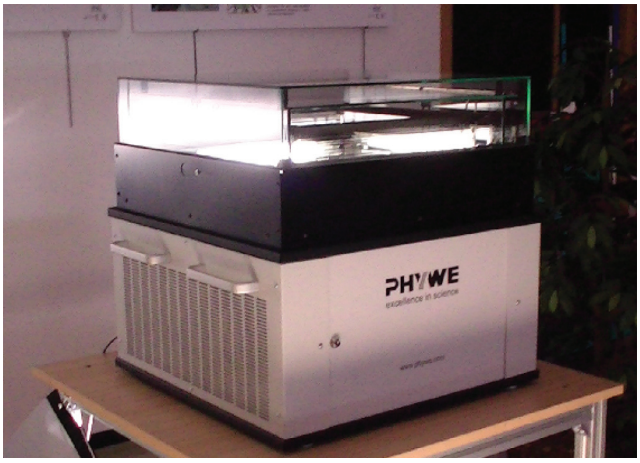

Fig. 2. (Color online) View of the diffusion cloud chamber constructed by PHYWE (Ref. 17).

III. THE IFIC CLOUD DIFFUSION CHAMBER

Our diffusion cloud chamber was purchased from the PHYWE Company.[17] It consists of a base and an observation volume on top of the base. The base comprises a cooling element, a power supply, an alcohol reservoir, a pump, and a programmable switch. A view of the chamber is shown in Fig. 2.

The observation volume (see Fig. 3) contains at the bottom a black metal plate of 40 cm $\times$ 40 cm, cooled to a temperature of about -35°C. At the top of the observation volume, a grid of electrical wires is located to slightly overheat the upper part of the chamber to ≈ 35°C. The grid also generates an electrical field, which is necessary to eliminate ions from the observation volume. Isopropyl alcohol from a reservoir is pumped into a gutter at the top of the observation volume of the chamber, where the heated wires ensure alcohol evaporation and diffusion. After condensation, alcohol drops fall into the bottom of the observation volume and flow back into the reservoir. Because the observation volume

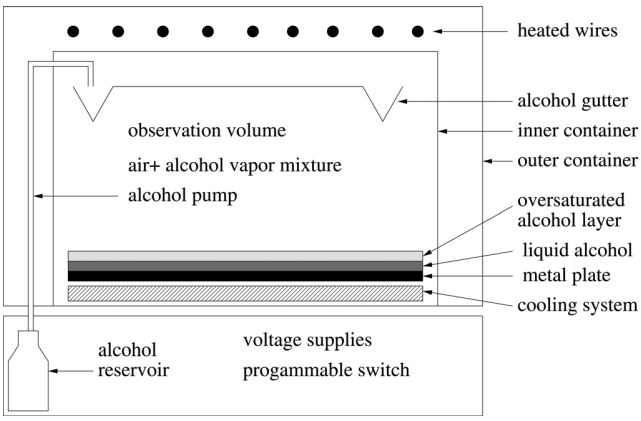

Fig. 3. Schematic view of the observation volume of the diffusion cloud chamber.

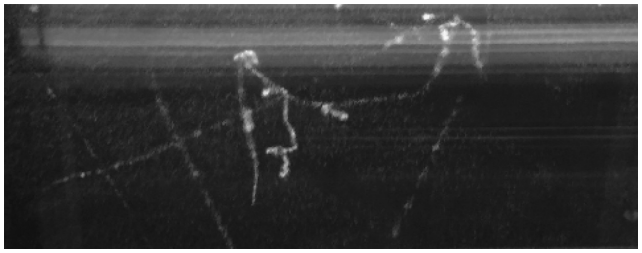

Fig. 4. Picture of a typical event seen with the diffusion cloud chamber. Observed tracks are produced by low energy electrons or muons.

is about 15 cm high, the temperature gradient is 4.7°C/cm. The supersaturated vapor layer is formed just above the metal plate, and has a thickness of ≈ 5 mm. The diffusion cloud chamber is not hermetically sealed, allowing the penetration of ambient air.

This diffusion cloud chamber is located in a large hall inside the experimental building of our institute. The hall is in the first floor of the building and has no direct ventilation source. However, it is surrounded by ventilated offices. Ventilation is turned off at night and during weekends. These details are relevant in order to compare our results with existing indoor measurements. Radon concentrations vary significantly, depending on the location of the measurement, and on heating, ventilation, and weather conditions.

IV. MEASURING RADON ABUNDANCE WITH A DIFFUSION CLOUD CHAMBER

The fact that radon decays in air can be observed in diffusion cloud chambers is mentioned in Ref. 14, but, to our knowledge, our measurements represent the first time that radon concentration in air using a diffusion cloud chamber has been discussed. As discussed in the following, this technique is faster and simpler than traditional techniques such as the charcoal method. It might be less accurate, and the diffusion cloud chamber cannot be transported easily. But simplicity, and the fact that radon decays are observed directly and not indirectly as is done with ^{214}Pb and ^{214}Bi gamma decays in the charcoal method, makes the diffusion cloud chamber measurement especially suitable for physics demonstrations to high school and university students. The key to understanding why the technique works will be discussed by discussing two pictures in Figs. 4 and 5.

Figure 4 shows a typical event seen in the chamber. There are several low density tracks, some of them with almost straight trajectories, and others suffering large angle scattering. They are produced by electrons and muons from cascades originating in secondary interactions of primary cosmic rays (typically protons) entering the upper part of the Earth's atmosphere. Figure 5 shows in the upper right corner a very short and dense track, very different from those in Fig. 4. These dense tracks occur at an average rate of 1 every 3 s, and can easily be counted, even with a standard watch. The maximum track length is about 5 cm and the typical thickness is 5 mm. Both properties imply that these tracks correspond to α particles, with a maximum range of about 5 cm in air for energies of about 5 MeV, as in radon decays. The high density of the track also implies a low speed and highly ionizing particles, as expected for α particles from radon decays ($v/c = 0.052$). According to Bethe–Bloch theory, the ionization energy loss by non-relativistic charged particles is proportional to Q^2/v^2, where Q is the electric charge and v the speed.[18] This dependence on Q and v is the reason why low speed α particles ($Q = +2$) are highly ionizing and have a short range (a few centimeters), even inside a low density medium such as air. In contrast, relativistic particles like those shown in Fig. 4 have very large ranges in air (exceeding several hundred meters).

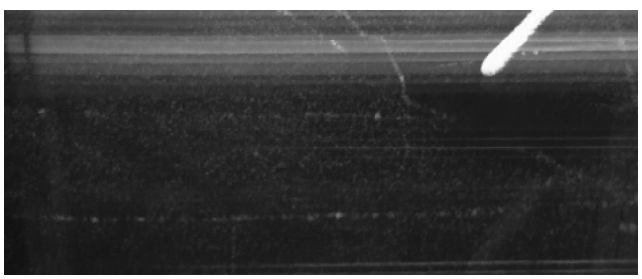

Fig. 5. Picture of an α particle from radon decay occurring in the diffusion cloud chamber.

Sometimes, dense tracks show up in double coincidences, which are also expected in the radon decay chain. In the following, we assume that all dense tracks observed are radon decays, or decays of one of the two polonium isotopes arising in the decay of ^{222}Rn. When the decay is perpendicular to the over-saturated layer, the track is shorter and can be confused with other interactions occurring in the chamber. This effect will be included as a systematic error in the calculation of the detection efficiency.

Various sets of radon decay measurements were performed with the diffusion cloud chamber during September and October 2010. Table II shows a set of measurements made in October 2010. The number of observed radon decays was recorded during 5 min at 9:30 AM and at 14:30 PM. This operation was repeated for three consecutive days. The values obtained are statistically equivalent. We did not observe any dependence on the day or the hour of the measurement. The average value is $N_0 = 75.7 \pm 3.5$ decays every $T_0 = 5$ min, where the error is only statistical.

To convert this measurement into a value for radon concentration in air, we need to take into account the dimensions of the black metal plate at the bottom of the chamber, L_x and L_y, and the thickness ℓ_z of the layer with over-saturated alcohol vapor. These values allow us to calculate the sensitive volume of the chamber, that is, the volume where α particles can be detected. We note that tracks observed in this thin sensitive layer (ℓ_z is only about 5 mm) originate mainly outside it. Because we are only interested in tracks produced inside the sensitive layer, we need a correction factor. This geometrical correction ϵ_{vol} is obtained by analytical calculations, or using a simple Monte Carlo program (see Appendix A). The analytical result is

Table II. Measurements of radon decays with the diffusion cloud chamber. The values shown are the number of counts during 5 min.

Day/Time	9:30	14:30
1 October 2010	82	74
4 October 2010	79	66
5 October 2010	73	80

$$\epsilon_{\mathrm{vol}} = \frac{\ell_z}{\ell_z + R/4}, \tag{2}$$

where R is the maximum length of α tracks in air. In our case, $\epsilon_{\mathrm{vol}} \approx 30\%$, because $R \approx 5$ cm.

The complete decay chain of ^{222}Rn is

$$^{222}\mathrm{Rn} \xrightarrow{\alpha} {}^{218}\mathrm{Po} \xrightarrow{\alpha} {}^{214}\mathrm{Pb} \xrightarrow{\beta} {}^{214}\mathrm{Bi} \xrightarrow{\beta} {}^{214}\mathrm{Po} \xrightarrow{\alpha} {}^{210}\mathrm{Pb}. \tag{3}$$

The isotopes ^{214}Pb and ^{214}Bi have β decays, yielding just low density tracks in the chamber and are of no practical interest here. The half-lives of the first five isotopes in this decay chain are 3.8 d, 3.1 min, 26.8 min, 19.9 min, and 164 μs, respectively, and imply that equilibrium is rapidly reached after a few hours. The isotope, ^{214}Po, decays further into ^{210}Pb, but the half-life of ^{210}Pb is 22.3 years. Therefore the decay chain is stopped for practical purposes after ^{214}Po decays into ^{210}Pb, although ^{210}Pb further decays until the stable isotope ^{206}Pb is reached:

$$^{210}\mathrm{Pb} \rightarrow {}^{210}\mathrm{Bi} \rightarrow {}^{210}\mathrm{Po} \rightarrow {}^{206}\mathrm{Pb}. \tag{4}$$

According to tabulated compilations,[19] the value of the α particle range R in air at 0°C is 3.9, 4.5, and 6.6 cm for ^{222}Rn, ^{218}Po, and ^{214}Po, respectively, corresponding to energies of 5.5, 6.0, and 7.7 MeV. These three α decaying isotopes rapidly reach secular equilibrium, and thus the activity of the three isotopes per radon decay is the same, and the total number of α decaying isotopes observed in our diffusion cloud chamber would be $N_{\mathrm{iso}} = 3$. This conclusion should be modified for confined areas, because the number of radon daughters is reduced due to surface deposition. Based on data in Ref. 20 we estimate that the effective number of decaying isotopes per radon decay in our diffusion cloud chamber is $N_{\mathrm{iso}} = 2.7 \pm 0.3$. The details of this estimate are given in Appendix B. The average maximum decay length of α tracks is $R = 5.0 \pm 1.2$ cm, after calculating the average for the three isotopes.

We assume a global observation efficiency ϵ_{obs} for α tracks of 100%, with an estimated 10% error due to track confusion and miscounts. The activity of radon in air per unit volume is

$$N = \epsilon_{\mathrm{obs}}\epsilon_{\mathrm{vol}} \frac{N_0}{T_0} \frac{1}{L_x L_y \ell_z} \frac{1}{N_{\mathrm{iso}}} = \epsilon_{\mathrm{obs}} \frac{N_0}{T_0} \frac{1}{L_x L_y} \frac{1}{\ell_z + R/4} \frac{1}{N_{\mathrm{iso}}}. \tag{5}$$

Table III provides a summary of the parameters used and their systematic errors. As seen in Table III, the thickness ℓ_z of the diffusion cloud chamber sensitive layer has a very large error, but contributes only moderately to the total systematic error.

Using these values we obtain a radon concentration equivalent to an activity of

$$N = 33.7 \pm 1.7(5\%) \pm 9.1(27\%)\ \mathrm{Bq/m^3}, \tag{6}$$

where the first error is statistical and the second is systematic. This value is consistent with the average radon concentration measured all over Europe in confined areas. This concentration is of the order of $N = 40$ Bq/m^3. Note that our diffusion cloud chamber is located in a very large room on a first floor, without direct ventilation. We only observe a small increase of radon concentration of some 20% when ventilation is switched off during weekends or at night. Our measurement is confirmed by a comparison with another one made at the same place and time using the charcoal method. This measurement yields an activity of

$$N = 26.2 \pm 4.5(17\%) \pm 7.3(28\%)\ \mathrm{Bq/m^3}, \tag{7}$$

where the first error is statistical and the second is systematic. The charcoal measurement is an average over 24 h, whereas our measurement is an average over 30 min. As discussed, some difference is expected due to the increase of radon concentration when the ventilation is off. This effect should be at the level of 5%–10%, smaller that the total uncertainty of the measurement.

Our measurement is compatible with previous measurements in open and closed areas in Valencia,[21] yielding typical radon concentrations in the range of 30–40 Bq/m^3, with peak values of up to 1000 Bq/m^3 in a few very localized places.

Table III. Summary of parameters and systematic errors.

Parameter	Meaning	Value	Error
ϵ_{obs}	Observation efficiency	1.0	0.1
N_0	Counts measured in T_0	–	–
T_0	Observation time	5 min	–
L_x	Lateral length of diffusion cloud chamber	40 cm	2 cm
L_y	Lateral length of diffusion cloud chamber	40 cm	2 cm
ℓ_z	Sensitive layer thickness	5 mm	2.5 mm
R	Maximum length of α 's in air	5.0 cm	1.2 cm
N_{iso}	Number of α decaying isotopes	2.7	0.3

V. SUMMARY AND CONCLUSIONS

We have measured the concentration of radon in air in a large room located in the experimental hall of our physics institute. We use a novel technique to detect radon concentration in air by detecting α particles with a diffusion cloud chamber. This instrument, a variant of the Wilson cloud chamber, was invented approximately 60 years ago to detect charged particles, and is presently used only for physics demonstrations for high school and university students. Our measurement is compatible with average indoor measurements taken all over Europe, and with measurements taken in the Valencia region. It also agrees with a measurement performed with the more traditional activated charcoal canister method. The measurement requires understanding of physics concepts such as radioactivity, secular equilibrium, uranium decay chain, cosmic rays, detection of nuclear radiations, statistical and systematic errors in measurements.

ACKNOWLEDGMENTS

We are grateful to R. Rodríguez and the technical staff of IFIC for maintenance of the chamber. We thank J. L. Ferrero for providing the canisters used to measure radon activity with the charcoal method, F. Ballester and J. Vijande for

helpful discussions, and F. Martínez for helping to install the chamber. We finally thank F. Botella, director of our Institute, for facilitating the acquisition of the chamber.

APPENDIX A: GEOMETRICAL CORRECTION TO THE EFFICIENCY

To calculate the geometrical correction to the efficiency, we use the Monte Carlo method. This method relies on repeated random number generation to compute a mathematical quantity, typically an integral with complicated boundary conditions. In our case, random numbers are used to generate the parameters of segments describing α tracks. A few thousands of these segments are required to obtain the result. Once the segments are generated, they are easily classified according to the boundary conditions.

Figure 6 shows a schematic view of the diffusion cloud chamber. The over-saturated alcohol layer of thickness ℓ_z is shown in grey. In the computer code, α tracks are segments of fixed length R originating inside the observation volume ($z>0$). For practical purposes we can take the origin of the track, z_0, along the z axis such that $0<z_0<R+\ell_z$.

Both the origin and the direction of tracks are generated randomly. They are then classified into three categories: (1) Tracks that stay outside the grey layer. They cannot be observed in the diffusion cloud chamber and are of no interest here. (2) Tracks originating inside the grey layer (N_1). They can always be observed in the diffusion cloud chamber. (3) Tracks originating outside the grey layer that penetrates inside it (N_2). They are also observed in the diffusion cloud chamber, but should not be counted because the active volume is only the grey layer.

The geometrical efficiency correction corresponding to Eq. (2) is

$$\epsilon_{\mathrm{vol}}=\frac{N_1}{N_1+N_2}. \tag{A1}$$

For $\ell_z=5$ mm and $R=5$ cm, the Monte Carlo result is $\varepsilon_{\mathrm{vol}}\approx 30\%$.

This problem has an analytical solution. A summary of the analytical approach is the following. N_1 is proportional to ℓ_z, and N_2 is proportional to the integral,

$$N_2\propto\frac{1}{2}\int(1-\cos\theta_m)dz_0, \tag{A2}$$

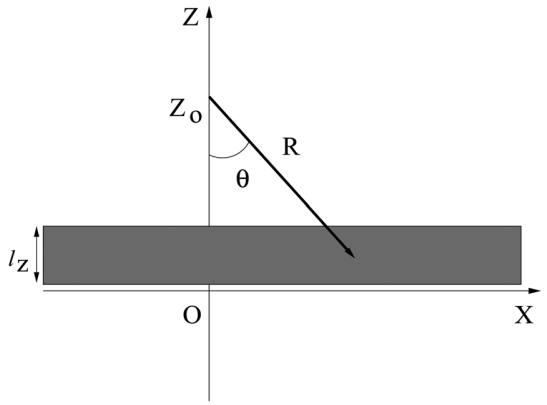

Fig. 6. Schematic view of the diffusion cloud chamber (vertical cut).

where $\cos\theta_m=(z_0-\ell_z)/R$ and θ_m is the maximum polar angle of a visible track. This integral should be calculated for $\ell_z<z_0<\ell_z+R$. The result is Eq. (2). It can easily be checked that Eq. (2) agrees with the MC result.

APPENDIX B: EFFECTIVE NUMBER OF α DECAYING ISOTOPES

The radioactive law for a decay chain of the type $I_0\rightarrow I_1\rightarrow I_2\rightarrow\ldots$ is

$$\frac{dN_i}{dt}=\lambda_{i-1}N_{i-1}-\lambda_iN_i-q_iN_i\qquad(i=1,2,\ldots), \tag{B1}$$

where N_i are isotope populations and λ_i represents decay constants. We modified these equations to account for the deposition of isotopes on surfaces by including deposition rates q_i. These rates are negligible for gases like radon, but are relevant for metals.

A typical example discussed in Ref. 20 is a room with a surface-to-volume ratio of 6 m^{-1} and deposition rates q_i of 7.3×10^{-4}, 1.2×10^{-4}, and 3.7×10^{-5} s^{-1} for ^{218}Po, ^{214}Pb, and ^{214}Bi, respectively. (We refer to these isotopes as RaA, RaB, and RaC, respectively.) The result, shown in the caption of Fig. 17 in Ref. 20 is the ratio of isotope activities per radon decay of 1/0.85/0.65/0.60 for Rn/RaA/RaB/RaC. Note that, in the absence of surface deposition, secular equilibrium is reached after a few hours and all isotopes would have the same activity. Because ^{214}Bi decays very rapidly into ^{214}Po, both isotopes have nearly the same activity. In this example the effective number of isotopes decaying into α particles per radon decay is

$$\begin{aligned}N_{\mathrm{iso}}&=A(^{222}\mathrm{Rn})+A(^{218}\mathrm{Po})+A(^{214}\mathrm{Po})\\&=1+0.85+0.60=2.45,\end{aligned} \tag{B2}$$

where A is the calculated activity per radon decay. For our diffusion cloud chamber the surface-to-volume ratio is larger (22 m^{-1}), but the concentration of alcohol vapor favors the attachment of metal isotopes to aerosol particles, increasing the value of N_{iso}. After recalculating the q_i factors and solving the decay equations, we find $N_{\mathrm{iso}}>2.4$. Because we know that $N_{\mathrm{iso}}<3.0$, we estimate $N_{\mathrm{iso}}=2.7\pm0.3$.

[a]Electronic mail: ramon.cases@uv.es
[b]Electronic mail: eduardo.ros@cern.ch
[c]Electronic mail: juan.zuniga@ific.uv.es

[1]H. Slätis, "On diffusion cloud chambers," Nucl. Instrum. **1**, 213–226 (1957).
[2]P. M. Blackett and G. Occhialini, "Photography of penetrating corpuscular radiation," Nature **130**, 363–363 (1932).
[3]L. G. Hoxton, "A permanent cloud chamber," Proc. Virginia Inst. **9**, 23–24 (1933–1934).
[4]R. E. Vollrath, "Continuously active cloud chamber," Rev. Sci. Instrum. **7**, 409–415 (1936).
[5]A. Langsdorf, "A continuously sensitive diffusion cloud chamber," Phys. Rev. **49**, 91–103 (1939).
[6]R. P. Schutt, "A theory of diffusion cloud chambers," Phys. Rev. **22**, 730–736 (1951).
[7]E. W. Cowan, "Continuously sensitive diffusion cloud chambers," Rev. Sci. Instrum. **21**, 991–998 (1950).
[8]R. P. Schutt, E. C. Fowler, D. H. Miller, A. M. Thorndike, and W. B. Fowler, "π^- p scattering observed in a diffusion cloud chamber," Phys. Rev. **84**, 1247–1248 (1951).
[9]W. B. Fowler, R. P. Shutt, A. M. Thorndike, and W. L. Whitemore, "Production of heavy unstable particles by negative pions," Phys. Rev. **93**, 861–867 (1954).
[10]A. Pais, "Some remarks on the V-particles," Phys. Rev. **86**, 663–672 (1952).

G Bibliography

- Document grande chambre à brouillard de diffusion PJ45/1
- Document LEP 5.2.04 about the visualisation of radioactive particle in a diffusion cloud chamber
- WebSite of IRNS about the origin of natural radioactivity
- Web site of ANDRA abour radioactivity
- Wikipedia in French about decay chains of natural radioactivity
- Passage of particles through matter, PDG review
- Python training at Subatech
- Root web site at CERN
- Python interface: PyROOT
- Site web SRIM
- Code de ce stage L3 sur GitHub)
- W.R. Leo, *Techniques for Nuclear and Particle Physics Experiments*, 2nd editions (1994), Springer-Verlag
- R. Cases, E. Ros and J. Zúñiga, American Journal of Physics 79, 903 (2011); doi: 10.1119/1.3591320